Journal of Geodynamics 149 (2022) 101890

Contents lists available at ScienceDirect

Journal of Geodynamics

journal homepage: www.elsevier.com/locate/jog

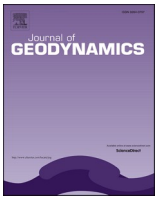

Jurassic-Cretaceous magmatic arcs in the Eastern Black Sea: Evidence from geophysical studies and 2D modeling

Tamara Yegorova [a,*], Valentina Gobarenko [b], Anna Murovskaya [a]

[a] Institute of Geophysics, National Academy of Sciences of Ukraine, Pr. Palladina 32, Kiev, Ukraine
[b] Institute of Seismology and Geodynamics, V.I. Vernadsky Crimean Federal University, Pr.Vernadskogo, 4, Simferopol, Russia

ARTICLE INFO

Keywords:
Magmatic arc
Subduction zone
2D gravity/magnetic modeling
Seismic tomography
Lithosphere
Black Sea

ABSTRACT

The origin, tectonic development, and lithosphere structure of the East Black Sea Basin (EBSB) are governed by the evolution of the northern branch of the Tethys ocean. The most spectacular features of its evolution could retain their imprints in geophysical fields and models, which we used to constrain a geophysical transect for the crust and upper mantle crossing the EBSB and the Shatsky Ridge (SR) from the Eastern Pontides to the Northern Caucasus. 2D gravity and magnetic modeling, constrained by wide-angle seismic data, revealed thin high-density and high-velocity sub-oceanic crust of the EBSB with the Moho shallowing up ~20 km depth. A spectacular feature of the Black Sea magnetic field is the Alushta-Batumi anomaly (ABA) above the SR that could be an imprint of subduction-related Middle Jurassic magmatic arc, whereas the Cretaceous (in Eastern Pontides) magmatic arc manifests itself by a chain of magnetic anomalies on the southern shoreline of the Black Sea. The high-velocity heterogeneity, revealed by seismic tomography, could be an image of a slab due to Mesozoic (Middle Jurassic and Cretaceous) subduction of the northern branch of Neotethys ocean. It shows rather a flat subduction slab that plunges northwards from subcrustal depths south of Eastern Pontide to the depth of > 70–80 km below the SR. Middle Jurassic and Cretaceous subduction fronts are located closely in the region of Eastern Pontides, whereas the related magmatic arcs are spaced differently – over the SR for the Middle Jurassic arc and along the southern coastline for Cretaceous Eastern Pontide magmatic arc correspondingly. The latter could be caused by the opening of the EBSB in the Cretaceous that separated the eastern segment of the BS onto the Eastern Pontides – Arkhangelsky Ridge and the SR – Northern Caucasus domains.

1. Introduction

The Black Sea (BS) region was formed as the result of the evolution of the Tethys ocean and its closure at the southern margin of Eurasia. During its evolution, the ocean has undergone several stages of shortening and closure. It occurred in the Late Triassic (Eo-Cimmerian event) during closing the Tethys and its subduction below the southern Eurasian margin (Golonka, 2004; Meijers et al., 2010; Nikishin et al., 2011; 2017; Okay and Nikishin, 2015; Saintot et al., 2006a; 2007; Simmons et al., 2018; Sosson et al., 2016). The strongest and most evident event occurred during the closure of the Neotethys ocean in the Late Cretaceous and its subduction below the Pontide magmatic arc that led to the opening of the backarc Black Sea Basin (Dercourt et al., 1993; Okay et al., 1994; Robinson and Kerusov, 1997; Nikishin et al., 2001, 2003).

Subduction-related magmatic arcs are usually associated with belts of magnetic anomalies along continental margins, sometimes related to gravity anomalies (Blakely et al., 2005; Williams and Gubbins, 2019). Such magnetic anomalies are specific features of the Northern Cascadia subduction zone in Canada, in Alaska, of buried magmatic arc in northern Japan, and of the Cretaceous magmatic arc of Antarctic Peninsula continental margin (Blakely et al., 2005; Clowes and Hyndman, 2002; Finn, 1994; Saltus et al., 1999; Yegorova et al., 2011). Thus, strong magnetic anomalies, usually of linear configuration or arc-shaped, and located along the coastline, are typical features of magmatic arcs. The magmatic arcs are formed by magmatic melts from subducting slab descending in the upper mantle that occurs at the depth of ~100 km. Magmatic arcs and associated magnetic anomalies are located at 70–170 km (sometimes up to 400 km) away from the subduction front at the surface (Blakely et al., 2005; Stern, 2002). Recent and ongoing subduction is accompanied by seismicity (Japan, Chile, and Cascadia subduction zones), whereas paleo subduction (paleo magmatic

* Corresponding author.
E-mail address: egorova@igph.kiev.ua (T. Yegorova).

https://doi.org/10.1016/j.jog.2021.101890
Received 2 June 2021; Received in revised form 22 November 2021; Accepted 9 December 2021
Available online 14 December 2021

arcs) shows no strong seismicity (Blakely et al., 2005; Contreras-Reyes et al., 2008). Recently, the idea that magnetic anomalies of magmatic arcs can be, at least in part, caused by hydrated serpentinized mantle wedge above the subducting slab is discussed in (Blakely et al., 2005; Williams and Gubbins, 2019).

The signs of subduction-related activity during Mesozoic time could persist in the magnetic field of the BS area that shows spectacular magnetic anomalies (Fig. 1B). One of them, called Alushta-Batumi anomaly (ABA), extends along its eastern (Caucasian) BS coast above the Shatsky Ridge (SR) and Tuapse Trough. We assume that it could be related to the Jurassic magmatic arc as a result of subduction and closure of Neotethys ocean below the Eurasian southern margin.

To confirm this idea we thoroughly investigated the lithosphere structure on the cross-section of the East Black Sea Basin (EBSB) passing in the NE direction from the Eastern Pontides through the SR to the Greater Caucasus using the gravity and magnetic modeling based on crustal structure from refraction and reflection seismic studies, velocity distribution in the lithosphere from seismic tomography, and paleotectonic reconstructions. Performed integrated modeling for the eastern part of the BS will help to find new constraints for understanding the better tectonic evolution of the study area. Particular attention is given to the SR – a key and poorly investigated offshore unit associated with the strong and extensive magnetic anomaly.

2. Geological and tectonic setting

The BS is an isolated deep-water basin surrounded by young Alpine structures. Its tectonic division is seen in the BS basement topography (Figs. 1a and 2a). Two deep basins with a highly thinned continental and/or oceanic crust are distinguished in the BS – the West Black Sea Basin (WBSB) and the East Black Sea Basin (EBSB). They are separated by a linear NW-oriented Mid Black Sea Ridge comprising the basement uplifts of continental crust of Andrusov Ridge on the north and Arkhangelsky Ridge on the south (Fig. 1a; Belousov and Vol'vosky, 1989; Finetti et al., 1988; Shillington et al., 2009; Starostenko et al., 2004; Tugolesov et al., 1985; Yegorova et al., 2010). The EBSB is framed by three Alpine fold belts: Southern Crimea (Crimean Mountains) and Greater Caucasus on the N and NE, and Eastern Pontides – Lesser Caucasus on the S-SE.

The BS basin is generally considered to be formed in a backarc setting in Cretaceous time due to subduction of the Neotethys ocean below the Pontide magmatic arc (Dercourt et al., 1993; Nikishin et al., 2001, 2003; Okay et al., 1994; Robinson and Kerusov, 1997). But the timing of opening the BS basins (or the age of oldest sediments), mechanisms of its formation, and crustal affinities, are still a matter of debate. Cretaceous age for the opening of the BS basin was inferred from onshore geological observations by Adamia et al. (1974), Letouzey et al. (1977), Görür (1988), and Nikishin et al. (2003). An Early Cretaceous to Palaeocene opening was deduced by Finetti et al. (1988) from seismic reflection data and corresponds with the concepts of Zonenshain and Le Pichon (1986) and Robinson et al. (1996).

Velocity structure of the lithosphere and paleotectonic reconstructions show that two basins in the BS have different affinity: formation of the EBSB could be genetically linked with the Transcaucasus domain in Northern Caucasus (Adamia et al., 1974; Golonka, 2004; Saintot et al., 2006a; Yegorova et al., 2010), whereas the WBSB was originated in a Eurasian setting, most probably, on the crust of Moesian platform due to rifting and strike-slip tectonics (Banks and Robinson, 1997; Hippolyte, 2002; Săndulesku, 1994; Seghedi, Oaie, 1994; Yegorova et al., 2010).

Between the EBSB and the Greater Caucasus fold belt, there is located the SR – an offshore continuation of the Transcaucasus with the basement of Baikalian and Palaeozoic age (Afanasenkov et al., 2007). Afanasenkov et al. (2007) suggest the occurrence of Middle Jurassic volcanics up to 2 km thickness in the SR since volcanic belt of that age (Bajocian mainly) is traced along the southern part of Greater Caucasus (drilled in the Rioni Basin in Georgia) and known in Eastern Pontides (Adamia, 2010; Meijers et al., 2010; Okay et al., 2014; Okay and Nikishin, 2015).

Westwards the SR, in the Crimean Mountains the Baijocian volcanics

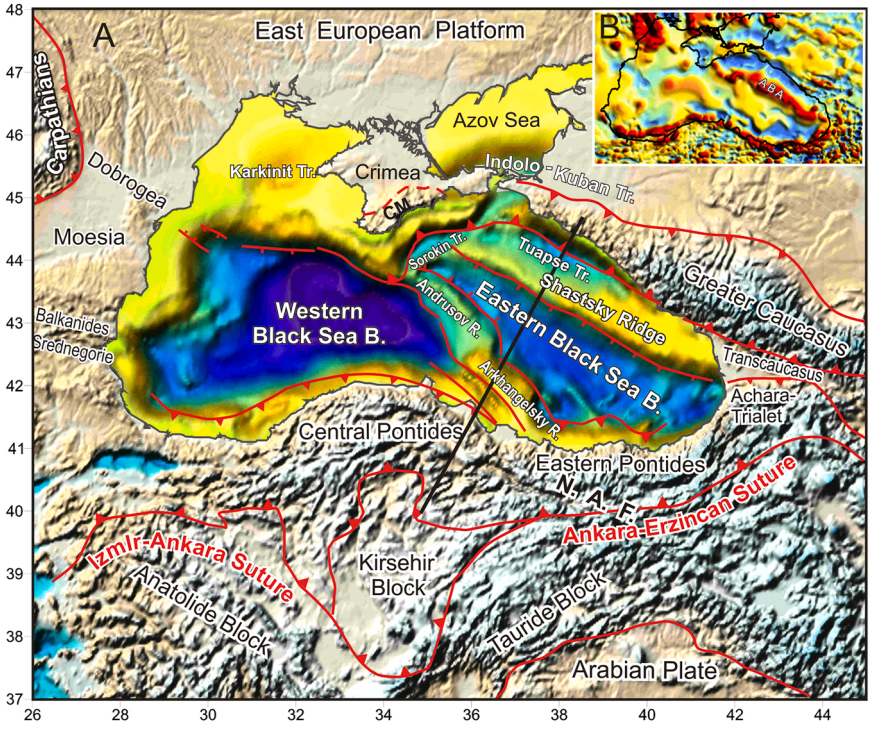

Fig. 1. Tectonic setting (A) and the magnetic field (B, insert) of the Black Sea and surrounding units. CM – Crimean Mountains, NAF – North Anatolian Fault. The depth map in the Black Sea shows the Cretaceous basement units according to Tugolesov et al. (1985). Magnetic map (B) shows the Alushta-Batumi anomaly (ABA) in the eastern part of the Black Sea above the Shatsky Ridge. Black solid line shows location of the interpreted profile.

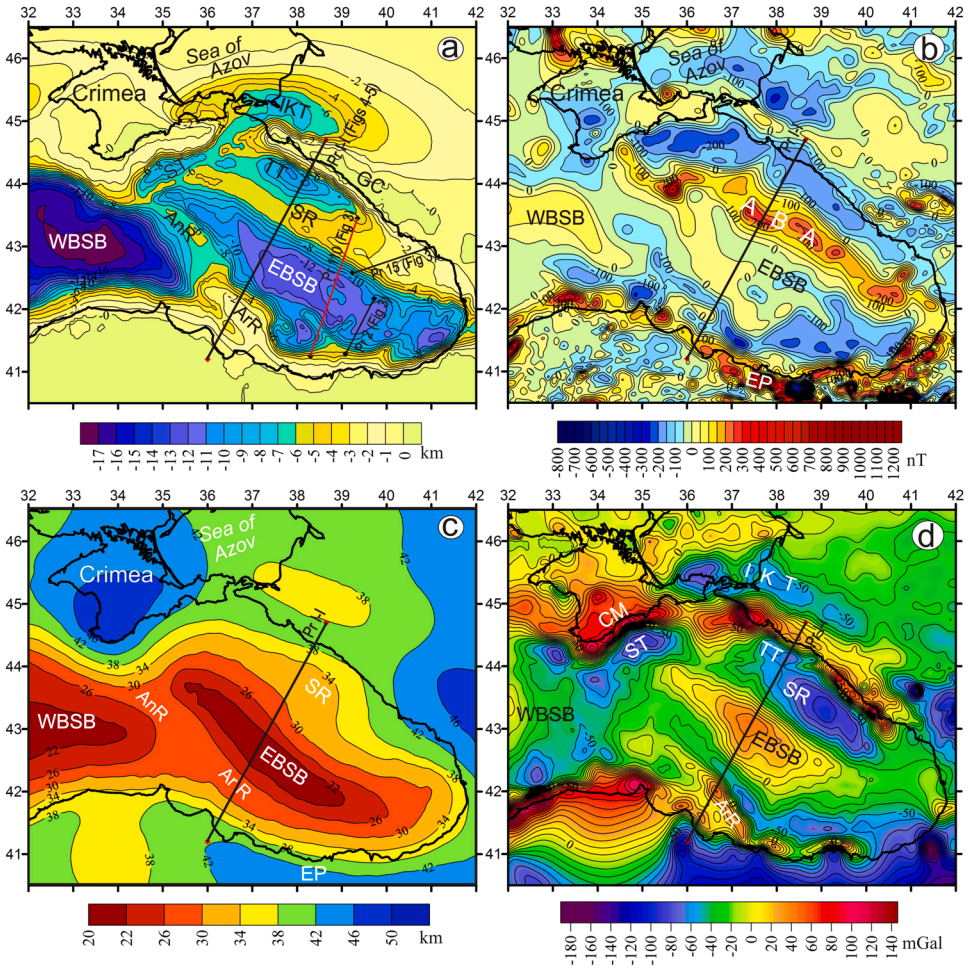

Fig. 2. Summary of crustal structure and potential fields in the area of the eastern part of the Black Sea: (a) depth of Cretaceous basement (Tugolesov et al., 1985), (b) magnetic field from the global model EMAG2 (http://www.geomag.org/models/emag2.htm), (c) depth to crustal base (Moho) (Grad and Tiira, 2009; Yegorova et al., 2013), (d) gravity field represented by Free Air anomalies offshore and Bouguer anomalies onshore) (Wybraniec et al., 1998). ABA – Alushta-Batumi anomaly, AnR – Andrusov Ridge, ArR – Arkhangelsky Ridge, EBSB – East Black Sea Basin, EP – Eastern Pontides, GC – Greater Caucasus, IKT – Indolo-Kuban Trough, SR – Shatsky Ridge, ST – Sorokin Trough, TT – Tuapse Trough. A solid black line shows the location of the interpretated line I-I (gravity and magnetic models). Black lines denote existed wide-angle refraction and reflection lines in the East Black Sea – pr. 15 (Baranova and Yegorova, 2020; Yegorova et al., 2020) and pr. 2 (Shillington et al., 2009). Multichannel deep seismic reflection profile 110 (Nikishin et al., 2015a) is shown by the red line.

of ~1-km thickness are developed (Afanasenkov et al., 2007). Several plutonic massifs mainly of Middle Jurassic age (and sometimes of Early Cretaceous age) are exposed within Southern Crimea; the most spectacular among them are Au-Dag, Kastel, and Kara-Dag plutons related to island arc formations (Meijers et al., 2010; Popov et al., 2018; Spiridonov et al., 1990a, b).

Thus, Afanasenkov et al. (2007) consider that along the southern edge of the Greater Caucasus could be developed the Middle Jurassic (mainly of Baijocian age) volcanic belt, which could be traced in the northern part of the SR and exposed on the surface in the Crimean Mountains and Eastern Pontides. So, it is supposed that before the EBSB opening, the Mid-Jurassic volcanic belt was a subduction-related magmatic arc – a unique entity of ~200 km width with a thickness of volcanics up to 4 km (Afanasenkov et al., 2007).

3. Initial data

The investigated cross-section I-I of ~440 km length, with the EBSB in its central part, passes from the SR and Northern Caucasus on NE to the Eastern Pontides on SW (Fig. 2). In the vicinity of the profile, the data are available on potential fields (gravity and magnetic), on the architecture of the sedimentary basin and velocity structure of the crystalline crust from deep seismic (reflection and refraction), as well as on velocity distribution in the lithospheric mantle from seismic tomography, which makes it possible to construct a velocity and density model for the crust and upper mantle and to conduct numerical modeling.

3.1. Gravity field

The gravity field of the EBSB is displayed in combined reduction (regional Bouguer anomalies onshore and Free-Air anomalies offshore) as a 5 × 5 km grid obtained by Wybraniec et al. (1998) within the framework of the EUROPROBE program. In the eastern part of the BS, an elongated in the NW direction gravity high of the EBSB (up to 40 mGal) is distinguished against the background of the negative gravity field of adjoining units (Fig. 2d). Among the latter, the gravity low of −90 mGal amplitude is seen above the Tuapse Trough and SR, located to the NW from the EBSB high. Deep sedimentary troughs along the northern margin of the EBSB – Sorokin and Indolo-Kuban Troughs are also caused gravity lows of −60 ÷ −80 mGal amplitude correspondingly (Fig. 2d).

The EBSB regional gravity field pattern is framed by chains of highs along the continental shelf edge and coastline. From the north, it constitutes the belt of gravity highs of Southern Crimea extending eastwards along the Caucasus coast. From the south, the EBSB is surrounded by a liner NW-trending high of the Arkhangelsky Ridge and by a chain of highs of Eastern Pontides (Fig. 2d).

2D and 3D studies are widely used to investigate the lithosphere structure below the BS. A 3D gravity back stripping analysis was performed to separate the gravity signals from different parts of the crust to obtain the mantle gravity anomalies (Yegorova and Gobarenko, 2010; Yegorova et al., 2013). These studies have shown good isostatic equilibrium of the deep structure of the EBSB, that is negative gravity effect of sediments almost totally compensated by the strong positive impact of the Moho shallowing up to ~20 km depth (Fig. 2a, c). 3D gravity analysis was also applied for the reconstruction of the Moho topography below the BS (Bilim et al., 2021; Starostenko et al., 2004). Gravity

calculations were applied by Entezar-Saadat et al. (2020) in their joint analysis of the lithosphere structure of the BS on a series of interpretation profiles.

3.2. Magnetic field

The most spectacular feature of the BS magnetic field is the Alushta-Batumi anomaly (ABA) of ~100–150 km width and ~600 km length, which extends along the SR (and Tuapse Trough) from Southern Crimea (c. Alushta) to SW Caucasus (c. Batumi) (Figs. 1b and 2b). Its nature is still debated (Gonchar, 2013; Malovitsky et al., 1972; Osipov et al., 1977; Shreider et al., 1997). Malovitsky et al. (1972) consider that the ABA could be related to a large fault that controlled the intrusion of magmatic melts of mafic and ultramafic composition. Its linearity, location between the Caucasus and the NE flank of the EBSB, as well as correlation with the gravity field pattern (Fig. 2b, d), could be indicative of its tectonic origin during the Mesozoic evolution of the eastern part of the BS area (Yegorova and Gobarenko, 2010). We consider that the shape and location of the ABA are similar to that of stripe magnetic anomalies of magmatic arcs formed by subduction of oceanic crust under the continental margin (Blakely et al., 2005; Clowes and Hyndman, 2002; Finn, 1994; Yegorova et al. 2011). The northern termination of the ABA in southern Crimea is explained by the occurrence of Middle Jurassic to Early Cretaceous volcanics (Kornev, 1982). The eastern prolongation of the Crimea anomaly into the Indolo-Kuban Trough is also explained by Middle Jurassic volcanics (Kornev, 1982).

The magnetic anomaly of Eastern Pontides is another specific magnetic anomaly of the East Black Sea region, which is traced onshore along the southern BS coastline and extends offshore westwards the Western Pontides (Figs. 1b and 2b). It consists of a series of separate anomalies of 200–300 nT magnitude that mark Pontide magmatic arc (Okay et al., 1994) formed in the Cretaceous at the southern Eurasian margin by closure/subduction of the Neotethys ocean (Barrier and Vrielynck, 2008; Okay et al., 2001).

3.3. Wide-angle reflection and refraction seismic study

Deep seismic profiling using refracted and wide-angle reflected waves, undertaken in the BS on the network of profiles in 60–80s of the last century, made the initial basis for studying the structure of the crust and upper mantle of the region (Malovitsky and Neprochnov, 1969; Moskalenko and Malovitsky, 1974; Neprochnov et al., 1970). These studies have established that the WBSB and EBSB are underlain by a thin high-velocity crust of oceanic and continental type with the crustal base (Moho interface) shallowing up to 20–25 km depth. To get additional information on the structure of the BS crust and, first of all, on the velocity distribution, a reinterpretation of seismic data on some of these existing lines has recently been undertaken using modern ray-tracing methods. In the eastern part of the BS region, these are profile 28–29 extending in ~N-S direction from the Sea of Azov through the northern and central part of the BS (Yegorova et al., 2010) and profile 15 intersecting the SR and the EBSB (Baranova and Yegorova, 2020; Yegorova et al., 2020). As a result, the structure of the crust was refined at the transition from the thin sub-oceanic crust of the EBSB to the SR continental crust (Baranova and Yegorova, 2020; Yegorova et al., 2020). It was found that the EBSB crystalline crust, covered by ~10 km-thick sediments with Vp ranging from ≤ 3.1 km s^{-1} to 4.0–4.5 km s^{-1} (Fig. 3a (right), Table 1), shows a thin (~ 10 km) high-velocity crust with a velocity varying from 6.5 km s^{-1} in the basement to 7.0 km s^{-1} on the Moho at 20–22 km depth. The SR has a continental crust of ~30 km thickness, with two layers – an upper crust as thick as ~15 km (Vp = 6.0–6.5 km s^{-1}) and a 10-km thick lower crust (Vp = 6.5–7.0 km s^{-1}), overlain by a thin sedimentary cover with Vp > 3 km s^{-1}. The transition from the continental crust of the SR to a thin sub-oceanic crust of the EBSB occurred rather dramatically, has a linear character in planar, parallel to the coastline of the eastern part of the BS, and is associated with the linear magnetic high ABA (Fig. 3a (right); Baranova and Yegorova, 2020; Yegorova et al., 2020).

Modern marine WARR (wide-angle reflection and refraction) studies were carried out in the EBSB on four profiles – one profile along the basin and three profiles crossing the EBSB with access to the Arkhangelsky Ridge (Scott et al., 2009; Shillington et al., 2009, 2017). They revealed a thin high-velocity EBSB crust of continental or oceanic type, bounded by the Moho shallowing to depths of 18–21 km below the basin, and the continental crust of the Arkhangelsky Ridge thickened to 28–29 km (Fig. 3a (left), Shillington et al., 2009, 2017). Obtained

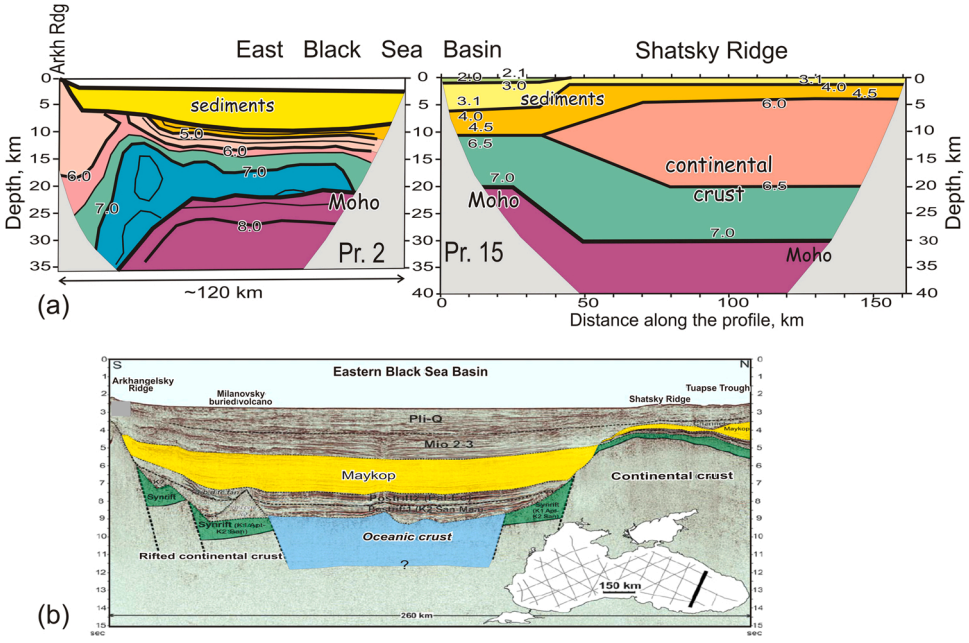

Fig. 3. Velocity structure of the East Black Sea Basin on wide-angle refraction profiles 15 (Baranova and Yegorova, 2020; Yegorova et al., 2020) and profile 2 (Shillington et al., 2009) (a), and multichannel reflection profile 110 (Nikishin et al., 2015a) (b). For the location of seismic lines see Fig. 2a. The numbers in (a) indicated P-wave seismic velocities in km s^{-1}. Arkh Rdg – Arkhangeksky Ridge.

Table 1
Physical parameters (seismic velocity, density and magnetic susceptibilities) used in the 2-D modeling on line I-I through the Eastern Pontides – Northern Caucasus.

	Layer	P-wave velocities, km s^{-1}		Density, g cm^{-3}		Magnetic susceptibility, SI	
		from Yegorova et al. (2010)	from Baranova and Yegorova (2019)	Initial model	Final model	Initial model	Final model
Sediments	Quaternary	1.6–3.0	2.0–2.1	2.10	2.10	0.0005	0.0005
	Pliocene-Miocene	3.0–3.2	3.0–3.1	2.35	2.35		
	Maykopian series (Lower.Miocene-Oligocene)	4.0–4.2	4.0–4.5	2.60	2.60–2.62	0.002	0.002
	Paleocene-Eocene	4.2–4.5		2.65	2.65		
Crust	Upper cont. crust	6.0–6.4	6.0–6.5	2.78–2.82	2.68–2.72	0.025	0.017
	Lower cont. crust	6.5–7.2	6.5–7.0		2.89–2.90		
	Crust of Shatsky Ridge			2.82	2.72 2.90	0.06	0.06
	Sub-oceanic crust	6.5–7.2	6.5–7.0	2.90–2.97	3.0–3.05	0.075	0.072
Upper mantle	'Normal' up. mantle	8.0		3.20	3.20		
	Low-density upper mantle of EBSB				3.12		

velocity models were interpreted in terms of an abrupt transition, coinciding with a transform fault, from magmatically poor to magmatically robust rifting along the strike of the EBSB (Shillington et al., 2009).

3.4. Deep multichannel reflection seismic

A deep seismic reflection study has been performed in the BS in 2011 within the framework of *Geology Without Limits* project. Totally 27 deep seismic reflection lines, of 8872 km length and seismic record up to 13 s, crossed major tectonic units of the BS (Graham et al., 2013). These data provide unique images of the deep structure of the continental margins and deep-water basins down to 20–30 km, sometimes reaching 40 km depth (Graham et al., 2013; Nikishin et al., 2015a, b). As a result, a map for the basement topography of the BS Basin has been updated (Nikishin et al., 2015a). The basement of the WBSB and EBSB includes areas with highly extended continental crust and areas of inferred oceanic crust (Nikishin et al., 2015a, b).

Fig. 3b shows that Late Cretaceous – Eocene deposits (deep-water carbonates, shales, and siltstones) on the Shatsky and Arkhangelsky Ridges appear very similar in the form of a series of subparallel bright reflections. There are indications of volcanic activity on the shoulders of the EBSB – on the SR and Andrusov Ridge. Nikishin et al. (2015a) suggested a possible Early Cretaceous (Albian?) volcanic arc along the SR, on which the EBSB was originated through rifting. Reflection seismic data of *Geology Without Limits* project were applied by Monteleone et al. (2019) and Maynard and Errat (2020) to study new deep structural and stratigraphic elements of the EBSB and to propose a new model for the evolution of the BS, and, in particular, of the EBSB.

4. Modeling the crustal structure on the cross-section I-I

4.1. Methodology of 2D gravity/magnetic modeling and parameterization of the model

3D modeling is the most appropriate approach for regional gravity studies. Such study, combined with seismic tomography, has been carried out for the Black Sea region (Yegorova et al., 2013). We used its general parameters of crustal structure and densities for developing the starting model for our 2D density modeling on line I-I crossing the EBSB (Fig. 1). Unlike the wide domain of the WBSB, the EBSB is a narrow slot rift up to 175 km width with 700-km length (Fig. 1), which gives us reason to fulfill the 2D modeling.

For 2D gravity and magnetic modeling, we used the software developed by Tchernychev and Makris (1996), which is based on the Talwani et al. (1959) algorithm and uses an approximation of the model by prisms. The prisms define the areas of constant density and magnetic susceptibility. In our case, the dimensions of prisms are 2×0.5 km^2 (X, Y) size for gravity and 2×0.25 km^2 – for magnetic calculations. Gravity calculations operate with relative densities, obtained by normalizing the absolute density values to a reference density. The magnetic bodies are located within the crust, bounded below by the Curie isoterm, which is estimated in the BS region at the depth of the crustal base (Moho interface) (Kutas et al., 1998; Starostenko et al., 2014; Verzhbitsky, 2002). During the modeling we set the extension of the structures crossed by the profile.

The geometry of the initial density and magnetic models is constrained by seismic reflection study and velocity models on seismic refraction profiles in the BS (Baranova and Yegorova, 2020; Tugolesov et al., 1985; Yegorova et al., 2010, 2013, 2020). For sediments we used the geometry of the sedimentary strata consisting of four layers – 1) Quaternary, 2) Pliocene-Miocene, 3) Maykopian series (Lover Miocene-Oligocene), 4) Paleocene-Eocene, taken from maps of Tugolesov et al. (1985) and used in the 3D gravity analysis for the BS (Yegorova et al., 2013). The structure of the crystalline crust on the interpreted cross-section is constrained by the velocity model on recently reinterpreted DSS profile 15 crossing the EBSB and the SR (Fig. 3; Baranova and Yegorova, 2020) and WARR profiles 2 and 3 that cross the EBSB and Arkhangelsky Ridge (Shillington et al., 2009), and takes into account the general 3D structure of the EBSB from (Yegorova et al., 2013). The Moho depths were taken from integrated 3D gravity and seismic tomography models of the Black Sea (Yegorova et al., 2013).

Density parameterization of the started model of the cross-section was made by conversion of P-wave velocities of the seismic models into densities (Table 1) using the conversion function of Ludwig et al. (1970) with taking into account Nafe and Drake (1963) and empirical functions between Vp and density of Birch (1960, 1961). The table shows also magnetic susceptibilities for crustal layers of our model, which takes into account available data from laboratory measurements and modeling (Telford et al., 1976). During the modeling, the geometry of the sedimentary layers and the crystalline crust, constrained by seismic models, were fixed. Further refinement of the models in Figs. 4 and 5 was achieved interactively with a better fit between calculated and observed potential fields employing changing the densities and magnetic susceptibilities in the layers and bodies of the model (the total number of iterations is up to 10). The values of densities and magnetic susceptibilities of key unites of the model were counter checked with linear inversion option that is offered by the software used.

4.2. Density model

The cross-section I-I goes close to the reflection line 100 (Nikishin et al., 2015a) and WARR profile 3 (Shillington et al., 2009) and takes into account combined velocity cross-section for the crust of the EBSB (Fig. 3a; Baranova and Yegorova, 2020; Yegorova et al., 2020) located SE from our interpretation line. The gravity field on line I-I shows a clear

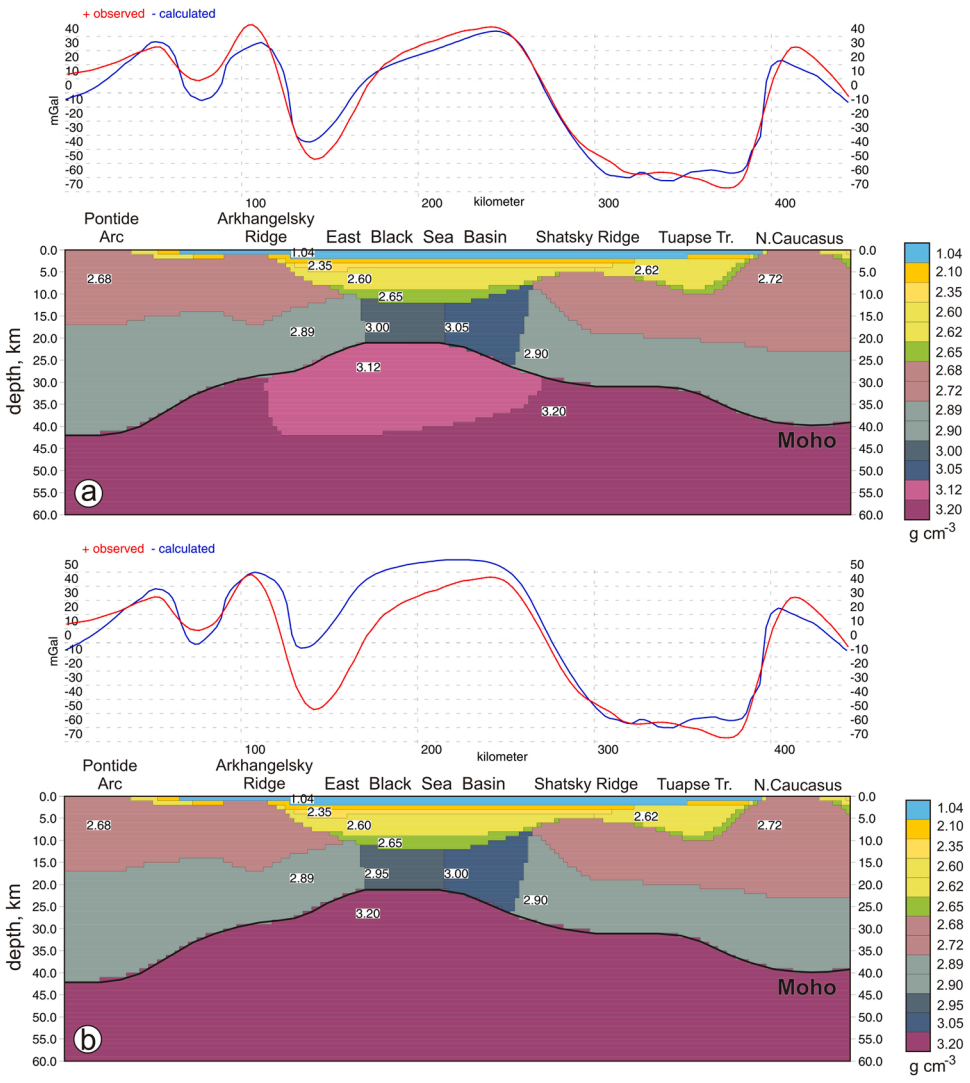

Fig. 4. Density models for the final version (a) and initial version (b) of the crust and upper mantle structure of the East Black Sea Basin on the line I-I passing from the Northern Caucasus to Eastern Pontides (for location see Fig. 2). Observed and calculated gravity are shown in the upper parts of the models. The density model represents the density values in the layers in g cm^{-3} (see also Table 1). The geometry of the model is constrained by the 3D crustal model of the Black Sea (Yegorova et al., 2013) and takes into account profile 15 (Baranova and Yegorova, 2020).

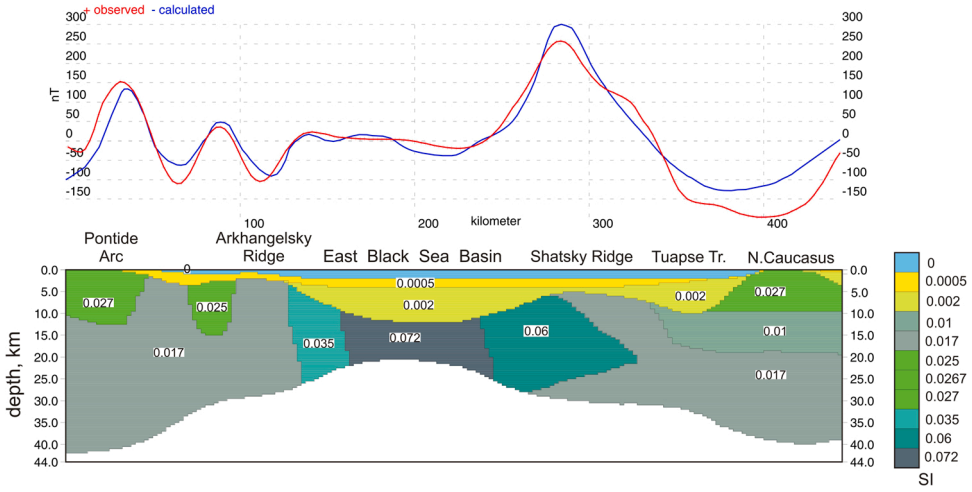

Fig. 5. Magnetic model for the crust of the East Black Sea Basin on line I-I passing from the Northern Caucasus to Eastern Pontides (for location see Fig. 2). Observed and calculated anomalies are shown in the upper panel. The geometry of the model is constrained by the 3D crustal model of the Black Sea (Yegorova et al., 2013) and takes into account the profile 15 (Baranova and Yegorova, 2020). Numbers in the cross-section indicate magnetic susceptibilities in SI units.

anomaly of the EBSB of 40 mGal amplitude, which then passes northeastwards into the gravity low of the SR and Tuapse Basin, ending within the high (30 mGal) of NW Caucasus (Fig. 4). Southwestwards of the EBSB, the line goes to the area of the positive gravity field of the Arkhangelsky Ridge and Eastern Pontides.

Fig. 4 represents the density models on line I-I. Our initial model (Fig. 4b) incorporates densities of 2.95–3.0 g cm^{-3} in the sub-oceanic crust of the EBSB (Table 1). It shows the misfit of 20–40 mGal between calculated and observed gravity indicating a possible additional input from the uppermost mantle, which was realized in the final model. The final density model with rms = 9.8 mGal is shown in Fig. 4a. It represents thin sub-oceanic crust of the EBSB juxtaposed between two blocks of continental crust – the Arkhangelsky Ridge – Eastern Pontids on the S and the SR – Northern Caucasus in the NE. The EBSB, with ~2 km-thick seawater layer, is filled with Cenozoic and younger sediments to a depth of ~12 km, which comprise thin Quaternary and Pliocene-Miocene deposits with densities (σ) of 2.10 g cm^{-3} and 2.35 g cm^{-3} correspondingly, thick (5–6 km) deposits of Maykopian series (Lower Miocene – Oligocene) with σ = 2.6 g cm^{-3} and metasedimentary rocks of the Eocene-Paleocene (σ = 2.65 g cm^{-3}).

A gravity high of the EBSB corresponds to thin crust with the Moho shallowing to ~22 km (Fig. 4). Final gravity model has shown that the density of the EBSB crystalline crust should be in the range of 3.0–3.05 g cm^{-3} (Fig. 4a). At this, higher density has been obtained in the NE part of the basin corresponding to a higher amplitude of the gravity high.

In the uppermost mantle of the EBSB a block of decreased to 3.12 g cm^{-3} density was modeled below the Moho, which could correspond with the presence of reduced velocities here revealed by the seismic tomography model (Figs. 6 and 7; Yanovskaya et al., 2016). Such areas of decompaction and low-velocity heterogeneity in the uppermost mantle are often observed under the rift zones (Achauer et al., 1994; Davis et al., 1993; Makris and Ginzburg, 1987; Prodehl et al., 1992). The reduced densities of the upper mantle below the sub-oceanic crust of the EBSB could be caused by presence of partly serpentinized ultrabasic rocks (partly serpentinized peridotites) in the upper mantle (Christensen, 1966), the presence of which in the upper mantle of the NNE sector of the BS adjacent to the Kerch and Taman Peninsulas (located to the north of our profile) was confirmed by local P- and S-wave tomography (Gobarenko et al., 2017).

Continental crust on both sides of the EBSB, of the SR – Northern Caucasus and Arkhangelsky Ridge – Eastern Pontides, are modeled by two layers – the upper crust with σ = 2.68–2.72 g cm^{-3} and the lower crust with 2.89–2.90 g cm^{-3}. The base of the continental crust (Moho interface) lies at the depth of 40 km and 42 km at the northeastern (Northern Caucasus) and southern (Pontides side) ends of the profile correspondingly (Fig. 4).

A vast gravity low of −60 mGal above the SR and superimposed Tuapse Trough is explained by a thick sedimentary sequence (7 km) of the Maykopian series (σ = 2.62 g cm^{-3}) of the trough overlapping the continental crust of the SR as thick as ~32 km (Fig. 4).

The transition from the continental crust of the SR to thin and high-

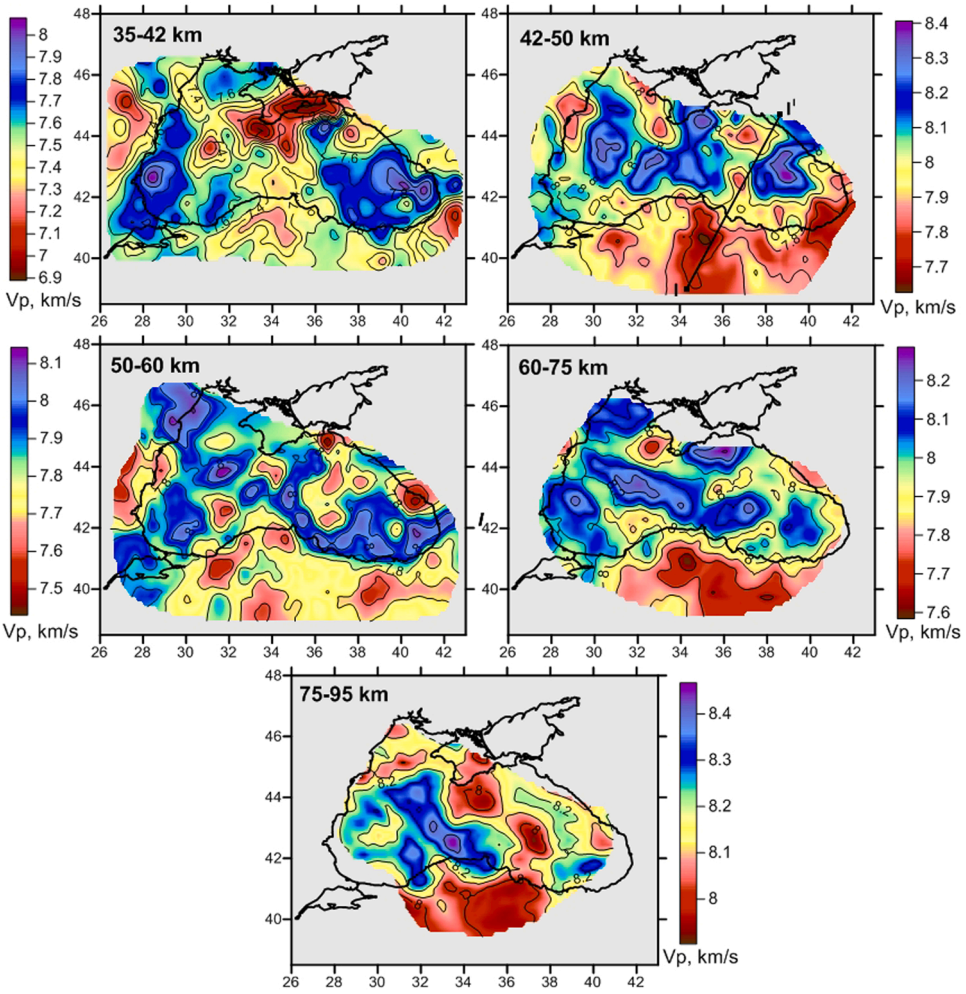

Fig. 6. Distribution of lateral variations of P-wave velocity (isolines in km s^{-1}) in the Black Sea lithospheric mantle at the depth of 35–95 km (data from Yanovskaya et al., 2016). The line I′- I′, which mostly coincides with the line I-I in Figs. 2, 4 and 5, shows the location of the vertical cross-section in Fig. 7.

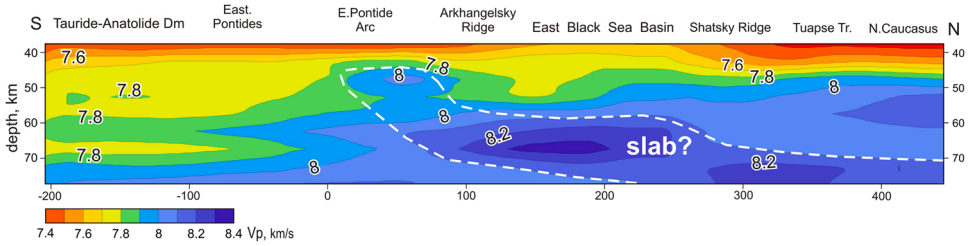

Fig. 7. The P-wave vertical cross-section on line I′-I′ (Fig. 6) showing the upper mantle structure from the Tauride-Anatolide domain through the East Black Sea Basin to the Northern Caucasus.

density EBSB crust occurs due to thinning of the upper crust until its complete disappearance (Fig. 4). The high density/velocity crust of the EBSB continues to trace on both sides of the basin as a lower continental crust with the density of ~2.90 g cm^{-3}. The high density/velocity crystalline crust of the EBSB may be the result of rifting due to stretching and thinning of the ductile lower crust, accompanied by intrusions of partially molten mantle substance of mafic and ultra-mafic composition, that could lead to crustal underplating and delamination (Furlong and Fountain, 1986; Li et al., 2010; Thybo and Artemieva, 2013; Thybo and Nielsen, 2009; Zhai et al., 2007). Moreover, these processes affected to a greater extent the NE part of the sub-oceanic crust of the EBSB adjacent to the SR (Fig. 4a).

4.3. Magnetic model

Line I-I crosses the mentioned above NW-trending magnetic anomaly ABA (250 nT) above the SR (Figs. 1b, 2b). To the SW, line I-I traverses close to zero magnetic field of the EBSB and ends at the Eastern Pontides (150 nT) magnetic anomaly. For magnetic modeling, we used the same crustal model, applied for density modeling. Fig. 5 shows the final magnetic model with the overal rms = 43 nT. The sedimentary cover comprises two layers – 1) Quaternary and Pliocene-Miocene and 2) Maykopian and Eocene-Paleocene successions with magnetic susceptibilities (æ) of 0.0005 and 0.002 SI correspondingly. Crystalline continental crust is modeled with æ = 0.02–0.027 SI (Fig. 5; Table 1). The thin crust of the EBSB of high velocity/density has the highest values of æ = 0.072 SI, which correspond to the magnetic susceptibility of rocks of mafic composition (Airo, 2005; Hunt et al., 1995; Telford et al., 1976). The magnetic bodies in the thinned central sector of the crust show the NE dip (towards the Northern Caucasus) that is considered to be a reliable feature, which in agreement with that of the EBSB crust and the SR.

Performed calculations have shown that ABA could be caused by a crustal body of ~90 km width, located in the SR crust and, in part, in the conjugate eastern part of the EBSB crust (Fig. 5). Modeled magnetic susceptibility (0.06 SI) indicates that could be caused by rocks of mafic to medium composition (Fig. 5). Eastwards the ABA goes over a stripe magnetic low reaching −200 nT, which is modeled by a superposition of non-magnetic sedimentary sequences of the Tuapse Trough, 10-km thick upper crust of the Northern Caucasus (0.027 SI) and located below a layer with æ = 0.01 SI down to the depth of 19 km (Fig. 5). The magnetic anomaly of Eastern Pontides of 150 nT at the southern end of line I-I is explained by an upper crustal body with æ = 0.027 SI indicative of the presence of intrusive rocks of medium composition (Airo, 2005; Hunt et al., 1995; Telford et al., 1976).

5. Seismic tomography

Lithospheric mantle below the BS has been studied by seismic tomography of the BS region using different data sets and inversion techniques (Gobarenko and Yanovskaya, 2011; Yanovskaya et al., 2016; Yegorova et al., 2013). Here we applied the model of Yanovskaya et al. (2016) that uses complete data set for the area of the BS and the Pontides, which is represented in Fig. 6 by five horizontal slices for the depth range 35–95 km. The uppermost section of this model (35–42 km) shows a domain with increased velocity (7.7–8.0 km s^{-1}) in the central, southern, and eastern segments of the eastern part of the BS, and a low-velocity domain (Vp ~7.1–7.3 km s^{-1}) around the Southern Crimea and Andrusov Ridge. The latter could be caused by the lower crust occurrence at these depths. The high-velocity domain continues to trace deeper (see sections at 50–60 and 70–75 km in Fig. 6) as an elongated in NW direction zone in the central and southern parts of the eastern BS. But it disappears at the deepest section (75–95 km) in contrast to the presence of an NW-trended high-velocity zone in the western part of the BS (Fig. 6).

A peculiar feature of the seismic tomography model is the low-velocity domain over the Pontides and Anatolide-Tauride Block, which is separated by gradient zone from the mentioned above the heterogeneous mantle of the BS. The transition from the Black Sea lithosphere to the low-velocity upper mantle of Pontides occurs dramatically along the coast: at depth of 50–60 km the velocity change from ~8.0 km s^{-1} to 7.7 km s^{-1} (Fig. 6).

We applied the tomography model in Fig. 6 to construct the velocity cross-section for the lithosphere on line I′-I′ for the 35–80 km depth range (Fig. 7). It shows a low-velocity domain (Vp = 7.6–7.8 km s^{-1}) below the EBSB at the depths of 35–55 km, under which, to a depth of 65–75 km, the upper mantle of the EBSB has increased (up to 8.2–8.3 km s^{-1}) velocities (Fig. 7). Low velocities (up to 7.6–7.7 km s^{-1}) in the uppermost part of the cross-section I′-I′ (at 35–43 km depth) were obtained in two blocks of continental crust–Eastern Pontides – Anatolian block in the SE and the SR – NW Caucasus in the NW, which could be indicative of the presence of the lower part of the continental crust at these depths.

In the region of the Pontide arc, an area of the increased velocity of 7.9–8.0 km s^{-1} is distinguished at 45–55 km depth. It is quite possible its connection with mentioned above high-velocity heterogeneity below the EBSB at the depth of > 60 km (Fig. 7). If so, this could be indicative of the presence in the upper mantle of a layer (slab ?) beneath the EBSB with a gentle NE dip, which starts just below the Moho in the area of Eastern Pontide, continuing on the depth of 60–75 km under EBSB and deepening to >70-80 km depth under the SR and NW Caucasus (Fig. 7). We did not calculate the gravity impact of this slab since its velocity increase of ~0.2 km s^{-1} could cause the gravity (~10–15 mGal) comparable or slightly higher the rms of the overal gravity model. Correspondingly, no fitted trend of this velocity fiature is visible in the gravity field, since highly anomalous and differentiated gravity field along the profile masks the weak signal from the upper mantle, detected by seismic tomography.

To the south of the Pontide arc, there is a sharp transition to a low-velocity upper mantle (Vp = 7.7–7.9 km s^{-1}, Fig. 7), which is characteristic of the young and heated Anatolian plate with high values of terrestrial heat flow (Aydin et al., 2005; Tezcan, 1995).

6. Discussion

Deep seismic reflection study (Graham et al., 2013; Nikishin et al.,

2015a, b) and reinterpreted refraction seismic profiles in the EBSB (Baranova and Yegorova, 2020; Yegorova et al., 2020), used for interpretation of potential fields and 2D modeling, together with seismic tomography study, made it possible to construct a geophysical transect on lines I-I and I′-I′ through the EBSB and SR from the Eastern Pontides to Northern Caucasus (Fig. 8) and to make their tectonic interpretation (Figs. 9–11). Herein we discuss the lithosphere structure of main units crossed by the transect in the context of tectonic evolution of the study region during the Mesozoic-Cenozoic time.

6.1. Shatsky ridge

The SR segment includes the ridge itself and the superimposed Tuapse Basin. The 3.5 km-thick sediments above the ridge, where non-compacted successions of Quaternary and Pliocene-Miocene age prevail, outline a dome structure of the SR basement (Figs. 3–5; Nikishin et al., 2015a, b, 2017). Whereas the Tuapse Basin is filled mostly with compacted sedimentary rocks of Maykopian series (Afanasenkov et al., 2007; Nikishin et al., 2015a, b, 2017) with thickness up to 6.5–7 km and density of 2.62 g cm^{-3}, which cause quite wide gravity low of −65 mGal (Fig. 4). The 32-km thick crust of the SR and Tuapse Basin is modeled by two layers (Figs. 3 and 4; Baranova and Yegorova, 2020): the upper crust with Vp = 6–6.5 km s^{-1} and σ = 2.72 g cm^{-3}, and a 10-km thick lower crust with Vp = 6.5–7.0 km s^{-1} (close to those in the crystalline crust of the EBSB) and 2.90 g cm^{-3} density (Figs. 3 and 4). Such crustal structure is in agreement with the results of multichannel seismic study and combined study of the lithosphere structure of the BS (Cousins and Wrobel-Daveau, 2018; Entezar-Saadat et al., 2020; Graham et al., 2013; Nikishin et al., 2015a, b).

General paleotectonic setting for the BS region for Mesozoic-Cenozoic time is presented in special atlases (Barrier and Vrielynck, 2008; Barrier et al., 2018; Dercourt et al., 2000) and discussed in many papers (Okay et al., 1994; 2001; Okay and Nikishin, 2015). Here we follow mainly the reconstruction model of Nikishin et al. (2015b), based on interpretation of new deep multichannel seismic lines in the BS, which infer that in the late Jurassic, before the EBSB opening, in the rear of the Jurassic subduction zone there was a vast carbonate platform occupied by an ensemble of present-day units of Eastern Pontides, Andrusov Ridge and Shatsky Ridge (Afanasenkov et al., 2007; Nikishin et al., 2015b).

The special position and nature of the SR are emphasized by its relation to the ABA – the most spectacular and extended magnetic anomaly of the BS (Figs. 1b and 2b). We assume that it could be related to linear magnetic anomalies of a subduction-related magmatic arc. Such island-arc belts are characterized by strong magnetic anomalies, which usually have linear or arc shapes, and are often accompanied by striped gravity anomalies (Blakely et al., 2005; Clowes and Hyndman, 2002; Finn, 1994; Grow and Bowin, 1975; Yegorova et al., 2011). The ABA is comparable to anomalies observed over the Kitakami batholith in Japan (Finn, 1994), the Peninsular Ranges batholiths in California and Baja California and the Antarctic Peninsula magmatic arc (Ferraccioli et al., 2006; Renner et al., 1982; Yegorova et al., 2011).

Thus, the ABA can be a manifestation of a magmatic arc formed during paleo-subduction of the Neotethys ocean beneath the Eurasian southern margin. The island-arc nature of the ABA is supported by its characteristics, such as linearity, long extension, high amplitude, and location. It is located roughly parallel to the NE of the palaeosubduction zone (Late Triassic – Early Jurassic) under the southern margin of Eurasia (Barrier et al., 2018; Meijers et al., 2010; Nikishin et al., 2017; Okay and Nikishin, 2015; Saintot et al., 2006a, 2007). We interpret it as related to the magmatic arc of the Early-Middle Jurassic age (Afanasenkov et al., 2007; Meijers et al., 2010; Nikishin et al. 2011). The magnetic modeling on line I-I revealed the occurrence of a magnetic body with the susceptibility ~0.06 SI in the crust of SR and, in part, in the transition to the EBSB (Figs. 5 and 8), which are characteristic of rocks of mafic to medium composition (Garrett, 1990; Hunt et al., 1995; Telford et al., 1976; Yegorova et al., 2011).

SR is thought to be a marine continuation of the Transcaucasus domain, the basement of which of Baikalian and Palaeozoic age comes to the surface in the Dzirula massif in Georgia (Adamia et al., 1974, 2007, 2017; Afanasenkov et al., 2007; Golonka, 2004; Saintot et al., 2006b). Along the southern zone of the Greater Caucasus, there is a Middle Jurassic (mainly Bajocian) volcanic belt, the main branch of which runs from the Dzirula massif to the SR. Thus, it is expected the widespread occurrence of the Middle Jurassic volcanics in the crust of the SR (Afanasenkov et al., 2007). Before the opening of the EBSB, there was a Middle Jurassic volcanic belt to the north of the subduction zone of the Neotethys ocean, which was a single entity reaching more than 200 km width with a thickness of volcanic rocks up to 1–4 km (Afanasenkov et al., 2007; Nikishin et al., 2011; Okay and Nikishin, 2015).

To the N-NW of the SR, there is located a fold-and-thrust structure of the Crimean Mountains that was formed during several Mesozoic orogenies on the boundary of the Triassic and Jurassic (mainly due to the Cimmerian tectogenesis). The western end of the ABA comes to the Crimean Mountains, which enables the identification of possible rock sources of this magnetic anomaly. The Early–Middle Jurassic stage of Cimmerian tectogenesis in Southern Crimea (Mileyev et al., 1992, 2006) was related to the emplacement of multiple Middle Jurassic plutons and

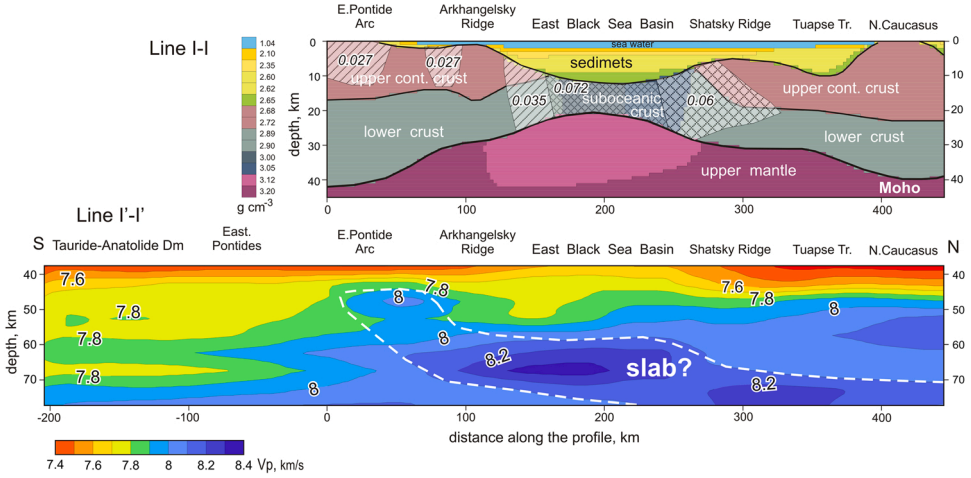

Fig. 8. Density/magnetic model for the crust of the study region on the line I-I (Figs. 2, 4 and 5) (upper panel) and P-wave velocity cross-section of the upper mantle on the line I′-I′ (Figs. 6 and 7). Domains with hatching on the upper panel show magnetic bodies with high and increased values of calculated susceptibilities (numbers in italic) from Fig. 5.

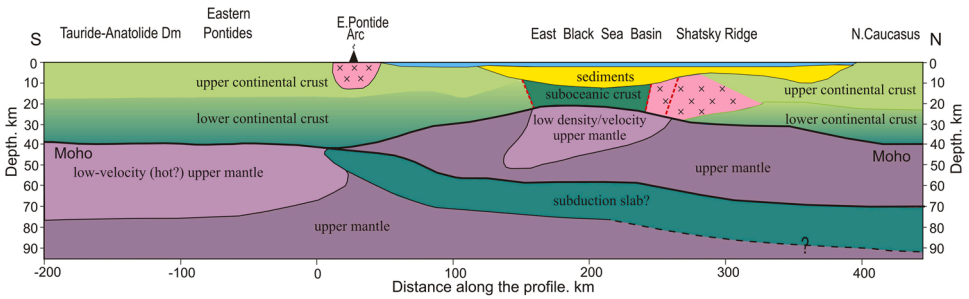

Fig. 9. Tectonic interpretation of gravity, magnetic and seismic tomography models (Fig. 8) for the crust and upper mantle on the line I′-I′ from the Tauride-Anatolide domain through the East Black Sea Basin to the Northern Caucasus showing the location of probable subduction slab and the Cretaceous (Eastern Pontides) and Middle Jurassic (Shatsky Ridge) magmatic arcs (shown by crosses).

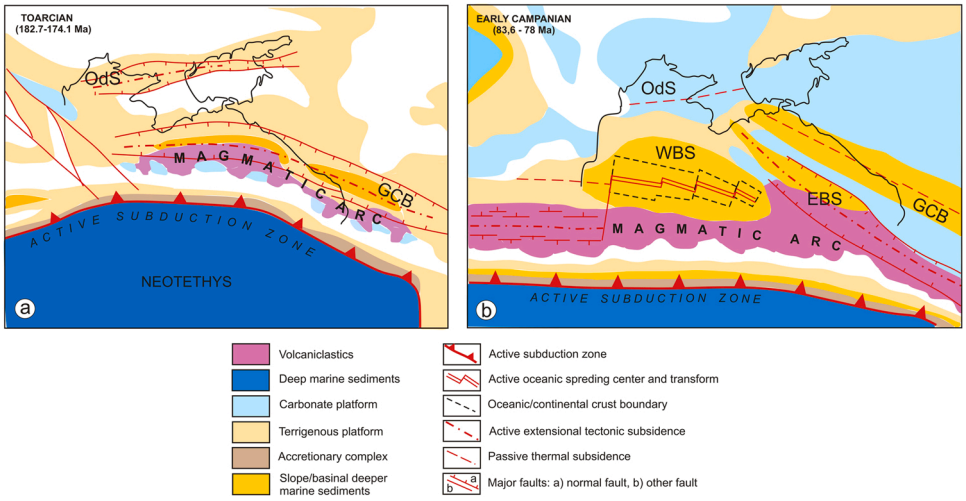

Fig. 10. Paleo-subduction zone configuration for the circum-Black Sea in Toarcian (a) and Campanian (b) (Barrier et al., 2018, modified). EBS – East Black Sea Basin, GCB – Greater Caucasus Basin, OdS – Odesa Shelf, WBS – West Black Sea Basin.

intrusions, which form the oriented in ~N-S direction the Pervomaisko–Ayu-Dag dolerite-gabbro–diorite complex (Spiridonov et al., 1990a, b; Meijers et al., 2010; Shniukova, 2019. The exposed in southern Crimea magmatic intrusions of Middle Jurassic age spatially fit with the high-velocity bodies revealed by seismic tomography in the upper-middle crust of Crimean Mountains (Gobarenko and Yegorova 2020a, b). Thus, intense magmatism reworked almost the entire crust of the Crimean Mountains, causing a significant gravity high and magnetic anomaly ABA (Yegorova et al., 2018; Gobarenko and Yegorova, 2020a, b).

The high-velocity body (Vp $\geq$ 8.2 km s^{-1}), detected by seismic tomography in the lithospheric mantle below the SR at the depth of > 70 km (Figs. 7 and 8), could be associated with the imprints of subduction activity. Namely, with a gently dipping in N-NE direction, below the Northern Caucasus, the remnant of the slab due to Jurassic (Early-Middle Jurassic) subduction of Neotethys ocean below the Eurasian southern margin, causing the magmatic arc, seen now in the region of the SR, and the magnetic anomaly ABA (Fig. 9; Barrier et al., 2018). Some similar aspects on the relation of Jurassic subduction and magmatic arc could be found in (Barrier et al., 2018; Dercourt et al., 2000; Hässig et al., 2020; Meijers et al., 2010; Nikishin et al., 2015b, 2017).

6.2. *Lithosphere of the East Black Sea Basin*

The generally accepted assumption that the crust of the BS could belong to oceanic type is based on the occurrence of thin (~10 km) high-velocity crystalline crust overlain by thick (10–12 km) Cenozoic and younger sediments and underlain by the Moho swallowing up to 20–22 km depth. If it is the case, the oceanic crust should rest on the oceanic lithospheric mantle. Seismic tomography study of the BS region has shown rather heterogeneous P-wave velocity structure of the BS upper mantle with two domains of increased velocity, different configuration, and velocity gradient beneath the western and eastern parts of the BS (Fig. 6; Yanovskaya et al., 2016; Yegorova et al., 2010, 2013). Integration of seismic tomography study and 3D gravity analysis revealed in western and eastern parts of the BS positive mantle gravity signal, suggesting that the BS basin is underlain by strong and cold lithospheric mantle, which is similar to the Precambrian lithosphere of the East European Platform (Yegorova et al., 2013). Similar results were obtained previously by regional gravity modeling for the European lithosphere (Kaban et al., 2010; Yegorova, Starostenko, 2002), and by calculating the integrated strength of the European lithosphere from the thermal model (Tesauro et al., 2009). This in agreement with the thermal state of the present-day BS lithosphere, which is rather cold that seen in extremely low values of surface heat flow and calculated deep temperatures (Gordienko et al., 2002; Kutas and Poort, 2008). A suggestion that the BS backarc basin formed within rheological strong continental lithosphere, probably assembled no later than Late Precambrian – Early Paleozoic times, was made by Stephenson and Schellart (2010) in their study of modern analogs of asymmetric slab roll-back models.

Thus the crust of the EBSB would not be a true 'oceanic' crust, but rather highly extended and intruded continental crust (and possibly contiguous deformed sedimentary strata), sometimes referred to as 'suboceanic' crust. Seismic tomography and gravity studies imply the

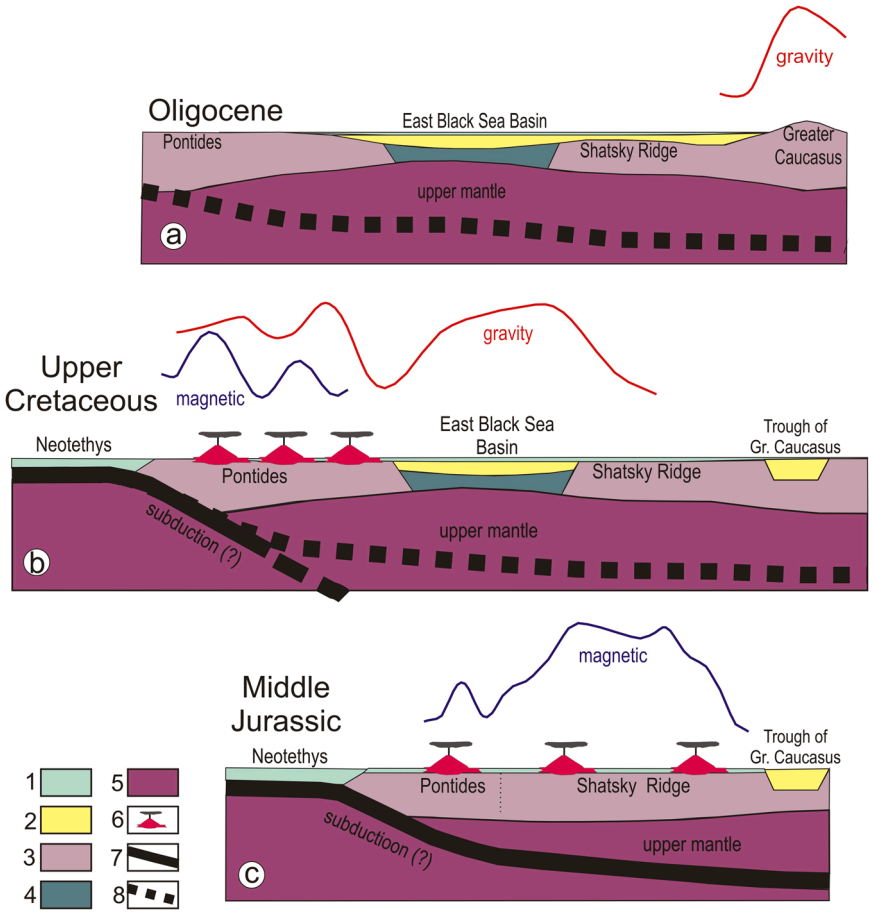

Fig. 11. Schematic illustration of a possible formation of Mesozoic magmatic arcs in the Eastern Black Sea area from Middle-Jurassic to Oligocene times with related geophysical anomalies (magnetic and gravity). 1 – sea water, 2 – sediments, 3 – continental crust, 4 – sub-oceanic crust, 5 – upper mantle, 6 – magmatic arc, 7 – active subduction (slab), 8 – relics of Jurassic subduction in (b) and of Middle Jurassic-Cretaceous subduction in (a).

absence of the asthenosphere below the BS at least a depth of 100 km (Yanovskaya et al., 2016; Yegorova et al., 2013) that corresponds to the LAB (lithosphere-asthenosphere boundary) in the BS in order 100–150 km (Artemieva, 2019; Artemieva et al., 2006; Cloetingh et al., 2003; Entezar-Saadat et al., 2020; Spadini et al., 1996; Tesauro et al., 2009; Yegorova and Gobarenko, 2010).

Thus, the question arises – how could be formed a thin crust of the BS overlain by thick sedimentary succession within strong continental lithosphere? We suppose that opening and rifting in the EBSB could occur, by the analogy with the that in the WBSB (Hippolyte et al., 2018), with involvement of polyphase process of continental rifting including stretching, thinning, and exhumation phases (Lavier and Manatschal, 2006; Péron-Pinvidic et al., 2007; Péron-Pinvidic and Manatschal, 2009). They identified two major extension-related detachments – 1) in the lower crust-upper mantle due to exhumation of mantle rocks along downward concave faults, and 2) in the basement – upper crust, which played a key role in rifting of deep magma-poor margins (Lavier and Manatschal, 2006; Péron-Pinvidic et al., 2007). In the western part of the BS, such crustal detachments were identified as low-velocity zones revealed on the wide-angle refraction profile 25 that cross the WBSB in ~N-S direction (Baranova et al., 2011; Hippolyte et al., 2018). The process that weakens the lithosphere during rifting involves attenuation of the upper-middle crust (mid-crustal weakening) in the initial stage of rifting, and, serpentinization of the lower crust – upper mantle leading to the formation of detachment surfaces (Lavier and Manatschal, 2006; Péron-Pinvidic and Manatschal, 2009).

The serpentinized upper mantle is inferred for the northern part of the EBSB from a local seismic tomography study showing low P-wave velocities with high P- to S-wave velocity ratios in the uppermost mantle underlain the thin sub-oceanic crust (Gobarenko et al., 2017). This is tentatively interpreted by Gobarenko et al. (2017) as representing serpentinized upper mantle of continental lithosphere exhumed during Cretaceous rifting and lithospheric hyperextension of the eastern Black Sea. The serpentinized upper mantle with similar parameters was found under central Japan, below small oceanic basins of the South China Sea, under the Amerasian part of the Arctic Ocean (Li et al., 2014; Kamiya and Kobayashi, 2000; Pease et al., 2014), as well as at the continental margin of the North Atlantic (Lundin, Dore, 2011). It seems likely that this phenomenon may also have occurred during hyperextension of the proto-Black Sea continental lithosphere.

Mechanisms of opening and rifting of the BS are still unclear. The WBSB is assumed to be opened during the southward drift of a continental block of the Istanbul zone along the transform faults at the western and eastern margins of the WBSB (Nikishin et al., 2003, 2011, 2015b; Okay et al., 1994; Robinson et al., 1996). For the narrow NW-trended EBSB two major models are proposed – one considering the counterclockwise rotation of the EBSB block (Okay et al., 1994) either the EBSB opened during clockwise rotation of the mid-Black Sea High (Robinson et al., 1996; Shillington et al., 2009). These models find further development in the model proposed by Hippolyte et al. (2018) for the BS basin. We prefer this model for opening and rifting of the EBSB based mainly on onshore data that accounts for the clockwise opening of the EBSB and a counterclockwise opening of the WBSB along transform faults at the eastern and western edges as a result of two asymmetric slab roll-backs of the Neotethys northward subduction plate (Hippolyte et al., 2018). Note here the model of Monteleone et al. (2019) of polyphase

evolution for rifting in the EBSB with evidence for rift propagation northwestwards associated with progressive basin opening.

6.3. Evolution of Middle Jurassic-Cretaceous magmatic arc in the Eastern Black Sea

The Mesozoic to Cenozoic evolution of the Black Sea region was subjected to the evolution of Tethys ocean at the Eurasian southern margin. Several subduction-related cycles are recognized during this evolution (Barrier et al., 2018; Dercourt et al., 2000; Nikishin et al., 2011; Saintot et al., 2006a; and references therein), which were governed by development, subduction, and closure of the Tethys leading to accretion of the Gondwana-derived Cimmerian terrains in Late Triassic (Early Jurassic?), and the migration of subduction (subduction retreat) followed by consumption of Permo-Triassic Tethys during the Jurassic–Cretaceous time. The final closure and subduction of the Neotethys in Late Cretaceous–Cenozoic times led to the opening of the back-arc BS behind the Pontide magmatic arc (Fig. 11).

The imprints of the most important tectonic events in the study area, such as magmatic arcs and subducting slabs could be preserved in potential fields (gravity and magnetic) and in the lithosphere structure as velocity heterogeneities revealed by seismic and seismology studies. As we discussed above, the ABA, the most spectacular magnetic anomaly of the BS region (Figs. 1b and 2b), could be related to anomalies of magmatic arcs, revealed and well studied in different subduction environments worldwide. In the BS region, it could be associated with the Middle Jurassic magmatic arc developed after the end of the Cimmerian orogeny in the Early Jurassic. In the Middle Jurassic, the subduction jumped south of the accreted complexes, and a magmatic arc was established along the southern margin of Eurasia (Okay and Nikishin, 2015). Palaeotectonic reconstruction maps infer the development of the Middle Jurassic subduction front along the present-day southern coast of the BS, whereas the Middle Jurassic magmatic arc is shown in the central and NW part of the present-day eastern segment of the BS (in the region of the SR) (Fig. 10a; Barrier et al., 2018; Dercourt et al., 2000; Nikishin et al., 2011; Okay and Nikishin, 2015). The explosions of Middle Jurassic volcanic and magmatic rocks are known around the eastern part of the BS – in Eastern and Central Pontides, Greater and Lesser Caucasus, and Southern Crimea, that permitted to distinguish the Middle Jurassic subduction-related magmatic arc traced for ~2800 km (Okay and Nikishin, 2015; Hässig et al., 2020). Study of Jurassic arc volcanism (using the 40Ar/39Ar isotope dating) in Crimea, a peninsula in the northern Black Sea, has shown that in the area prevail Middle Jurassic magmatic rocks (~172–158 Ma) (Meijers et al., 2010; Popov et al. 2018; Shniukova, 2019); the uppermost Jurassic to lowermost Cretaceous rocks (~151–142 Ma) have lesser distribution (Meijers et al., 2010). Both groups of rocks have a subduction-related geochemical signature (Meijers et al., 2010; Popov et al. 2018; Shniukova, 2019). Velocity cross-section of the upper mantle on line I′-I′ (Figs. 7 and 8), constructed from seismic tomography study (Yanovskaya et al., 2016), shows a high-velocity heterogeneity that starts near the Eastern Pontides, continue to trace at the depth of 60–75 km under the EBSB and below the SR to a depth of > 70–80 km. We infer this upper mantle velocity heterogeneity as an imprint of the Middle Jurassic subduction slab plunging in the N-NE direction below the Eurasian southern margin. In this case, subduction seems to be rather flat (Figs. 8, 9 and 11c). This corresponds with geochemical data and paleotectonic reconstructions providing evidence for Jurassic northward subduction below the Eurasian margin that requires flat-slab subduction, because the distance from Crimea to the trench, before Black Sea opening, is estimated at ~500 km (Barrier et al., 2018; Meijers et al., 2010; Shniukova, 2019).

Almost up to the end of the Jurassic, the area of the eastern part of the BS represented the carbonate platform at the southern margin of Eurasia limited from the north by the sedimentary basin of Greater Caucasus (Afanasenkov et al., 2007; Barrier et al., 2018; Dercourt et al., 2000). This vast carbonate platform comprised the present-day Eastern Pontides, Andrusov Ridge, and SR (Afanasenkov et al., 2007).

Further consumption of Neotethys occurred during the Cretaceous with the migration of active subduction to the south of Eastern Pontides and developing the Pontide magmatic arc, which is illustrated by the paleotectonic map in Fig. 10b (Barrier et al., 2018) and restoration of tectonic events at the southern margin of Eurasia in Fig. 11b. The Cretaceous magmatic arc along the BS southern coastline associates with a stripe of magnetic anomalies of much lesser magnitude than the ABA (Figs. 1b, 2b and 11b), and with a chain of residual (crust free) gravity anomalies (Fig. 12c in Yegorova et al., 2013). The magnetic model (Fig. 5) shows that the magnetic inhomogeneities of the Eastern Pontide arc localized mainly in the upper crust down to a depth of 12 km. Whereas the ABA is explained by a large crustal body under the SR with the magnetic susceptibility of 0.06 SI, spreading throughout the entire crystalline crust to a depth of 30 km. This maybe indicative of a more intense magmatic process in the Middle Jurassic (SR), which could have affected almost the entire crust than in the Cretaceous time (Pontide arc) (Figs. 5 and 11). In more detail, this process has been studied in Southern Crimean, where local seismic tomography detected bark saturation of the crust by high-velocity bodies, which correspond to exposed on the surface Middle Jurassic intrusive massifs and plutons of different compositions (Gobarenko and Yegorova, 2020a, b; Yegorova et al. 2018).

A continuous extensional magmatic arc was established in the late Cretaceous, coeval with the opening of the Black Sea as a backarc basin (Barrier et al., 2018; Okay and Nikishin, 2015). The position of the developed magmatic arc and the subduction front is shown in Fig. 10b for the Campanian time (Barrier et al., 2018). We believe that a high-velocity body in the subcrustal mantle in the Eastern Pontides region (Figs. 7–9) could be indicative of the presence of a slab (slab retreat) due to the Cretaceous subduction (solid black line in Fig. 11b), which further, as already noted, plunges northward under the EBSB and continues under the Shatsky Ridge, thus inheriting an earlier zone of heterogeneity formed during the Middle Jurassic subduction (dashed black line in Fig. 11a,b). In such a way, a single slab could be formed, wherein the allocated shallow segment could be related to Cretaceous subduction in the area of Eastern Pontide, and deeper segment, below the SR, – to the Middle Jurassic subduction (Fig. 11).

Both subduction fronts, formed in the Middle Jurassic and Cretaceous, are located very close in the region of Eastern Pontides and south of it, while the magmatic arcs are located differently. In the first case, the Middle Jurassic arc is located in the north-eastern and central part of the EBSB (approximately in the area of the SR), and in the second case, the Cretaceous magmatic arc occurred along the southern coastline of the BS. Thus, a conclusion could be made that Jurassic and Cretaceous subduction zones (the latter related to BS opening) worked in one zone at the Eurasian southern margin, that is, the younger subduction zone (Cretaceous) inherited the Jurassic subduction one (Fig. 11). Nikishin et al. (2011) show the Jurassic-Cretaceous subduction zone as a single zone located southwards of the Pontide magmatic arc. This point of view coincides with the model Hässig et al. (2020) on a single and continuous north dipping subduction throughout the Jurassic-Early Cretaceous along the southern Eurasian margin. At the same time, we do not rule out the possibility of occurrence of the slight roll-back subduction in the Early Cretaceous (Fig. 11b) that led to subduction front moved slightly further south (Fig. 10).

7. Conclusions

The Mesozoic-Cenozoic evolution of the East Black Sea Basin (EBSB) was subjected to the evolution of the northern branch of the Tethys ocean on the Eurasian southern margin. The imprints of the most important tectonic events are manifested themselves in geophysical fields (gravity and magnetic) and preserved in the lithosphere structure as velocity heterogeneities revealed by seismic (active and passive) studies. The new transect for the lithosphere of the eastern part of the

Black Sea (BS), crossing the EBSB from the Eastern Pontides to the Northern Caucasus, is constrained by comprehensive analysis of new and available geophysical data and modeling including seismic images and velocity models from deep seismic reflection and refraction studies, seismic tomography, as well as 2D gravity and magnetic modeling. The main results obtained by our study could be summarized as follows.

(1) A key unit of our study is the Shatsky Ridge – an offshore extension of the Transcaucasus domain, located between the Northern Caucasus and the EBSB and associated with the spectacular magnetic Alushta-Batumi anomaly (ABA), which is related to Middle Jurassic magmatic arc formed by closure of Neotethys ocean. Another magnetic anomaly along the southern shoreline of the eastern BS marks the Cretaceous Pontide magmatic arc originated due to the final closure of Neotethys ocean that led to the opening of the backarc EBSB at the rear of Pontide magmatic arc.
(2) The high-velocity heterogeneity, revealed in the upper mantle by seismic tomography, is interpreted, most likely, as an image of a slab formed due to Middle Jurassic and Cretaceous subduction phases. It shows rather a flat subduction slab that plunges in the northern direction from subcrustal depths in the region to the south from the Eastern Pontide arc through the upper mantle below the EBSB to the depth of > 70–80 km below the Shatsky Ridge.
(3) The subduction fronts – Middle Jurassic and Cretaceous are located very closely – in the region to the south of Eastern Pontides, whereas the related magmatic arcs occurred differently – the Middle Jurassic arc (associated with the ABA) locates mostly over the Shatsky Ridge, while the younger (Cretaceous) Eastern Pontide magmatic arc occurs along the southern coastline of the eastern Black Sea.
(4) Such a position of magmatic arcs is associated with the formation of the backarc EBSB, since before the opening of the latter, the eastern segment of the Black Sea was a carbonate platform occupied by present-day units of the Shatsky and Arkhangelsky Ridges, and Eastern Pontids, which, after the EBSB formation, were split and spaced on either side of the newly formed basin. Its continental crust as a result of extension and rifting, was strongly thinned and saturated with melts of mantle rocks, and overlain by a large thickness of sedimentary rift and post-rift successions, among which the deposits of Maykop series predominate.

CRediT authorship contribution statement

Tamara Yegorova: Conceptualization, Methodology, 2D gravity/magnetic modeling, Writing – original draft. **Valentina Gobarenko:** Methodology, Software. **Anna Murovskaya:** Visualization, Investigation, Interpretation of the results.

Declaration of Competing Interest

The authors declare that they have no known competing financial interests or personal relationships that could have appeared to influence the work reported in this paper.

Acknowledgments

The study was supported partially by the National Academy of Sciences of Ukraine (project III-21-17) and by the Russian Foundation for Basic Research (project 16-05-00996). We are grateful to two anonymous reviewers for their constructive comments.

References

Artemieva, I.M., 2019. Lithosphere structure in Europe from thermal isostasy. Earth-Sci. Rev. 188, 454–468. https://doi.org/10.1016/j.earscirev.2018.11.004.
Artemieva, I.M., Thybo, H., Kaban, K., 2006. Deep Europe today: geophysical synthesis of the upper mantle structure and lithosphere processes over 3.5 Ga. In: Gee, D.G., Stephenson, R.A. (Eds.), European Lithosphere Dynamics, 32. Geological Society, London, Memoirs, pp. 11–41.
Achauer, U., the KRISP Teleseismic Working Group, 1994. New ideas the 1985 and 1989–90 seismic tomography experiments. Tectonophysics 236, 305–329.
Adamia, S., 2010. Geological Map of Caucasus 2010, 1/1 000 000 scale. M. Nodia Institute of Geophysics, Tbilisi State University, Georgia.
Adamia, Sh, Chabukiani, A., Mikeladze, Z., 2007. Correlation of main tectono-sedimentary unites of the Eastern Black Sea and Caucasus-Eastern Pontides. In: Problematic Issues of Geodynamics, Petrology and Metallogeny in the Caucasus. Proceedings, Baku, pp. 36–49 (in Russian).
Adamia, S., Gamkrelidze, I.P., Zakariadze, G.S., Lordkipanidze, M.V., 1974. Adjara-Trialeti trough and the problem of the Black Sea origin. Geotectonika 1, 78–94.
Adamia, S.A., Chkhotua, T.G., Gavtadze, T.T., Lebanidze, Z.A., Lursmanashvili, N.D., Sadradze, N.G., Zakaraia, D.P., Zakariadze, G.S., 2017. Tectonic setting of Georgia – Eastern Black Sea: a review. In: Sosson, M., Stephenson, R.A., Adamia, S.A. (Eds.), Tectonic Evolution of the Eastern Black Sea and Caucasus, 428. Geological Society, London, pp. 11–40. https://doi.org/10.1144/SP428.6 (Special Publications).
Afanasenkov, A.P., Nikishin, A.M., Obukhov, A.N., 2007. Geology of the Eastern Black Sea. Scientific World, Moscow, p. 198.
Airo, M.-L. 2005. Regional interpretation of aerogeophysical data: extracting compositional and structural features. Geological Survey of Finland Special paper 39, 176–197.
Aydin, I., Karat, H.I., Kocąk, A., 2005. Curie-point depth map of Turkey. Geophys. J. Int. 162, 633–640. https://doi.org/10.1111/j.1365-246X.2005.02617.x.
Banks, C.J., Robinson, A., 1997. Mesozoic strike-slip back-arc basins of the western Black Sea region. In: Robinson, A.G. (Ed.), Regional and Petroleum Geology of the Black Sea and Surrounding Region, 68. AAPG Memoir, pp. 53–62.
Baranova, E.P., Yegorova, T.P., 2020. The crustal structure of the transition from the East Black Sea Basin to the Shatsky Ridge from the reinterpretation of deep seismic sounding data on profiles 14-15-16. Geophys. J. 42 (3), 59–77. https://doi.org/10.24028/gzh.0203-3100.v42i3.2020.204702.
Baranova, Y.P., Yegorova, T.P., Omelchenko, V.D., 2011. Detection of a waveguide in the basement of the northwestern shelf of the Black Sea according to the results of reinterpretation of the DSS materials of profiles 26 and 25. Geophys. J. 6 (33), 15–29.
Barrier, E., Vrielynck, B., 2008. Paleotectonic maps of the Middle East, Atlas of 14 maps, Tectonosedimentary-Palinspatic maps from Late Norian to Pliocene. Commission for the Geologic Map of the (CCMW-CCGM), Paris, France.
Barrier E., Vrielynck, B., Brouillet J.F., Brunet M.F. (Contributors: Angiolini L., Kaveh F., Plunder A., Poisson A., Pourteau A., Robertson A., Shekawat R., Sosson M., Zanchi A.), 2018. Paleotectonic Reconstruction of the Central Tethyan Realm. Tectonono-Sedimentary-Palinspastic maps from Late Permian to Pliocene. CCGM/CGMW. Paris, Atlas of 20 maps (scale: 1/15 000 000). ⟨https://www.ccgm.org⟩.
Belousov, V.V.Vol'vosky, B.S. (Eds), 1989. Structure and Evolution of Earth's Crust and Upper Mantle of Black Sea. Nauka, Moscow, p. 208 (in Russian).
Bilim, F., Aydemir, A., Ateş, A., Dolmaz, M.N., Kosaroglu, S., Erbek, E., 2021. Crustal thickness in the Black Sea and surrounding region, estimated from the gravity data. Mar. Petrol. Geol. 123, 104735 https://doi.org/10.1016/j.marpetgeo.2020.104735.
Birch, F., 1960. The velocity of compressional waves in rocks to 10 kilobars. Pt. 1. J. geophys. Res. 65 (4), 1083–1102.
Birch, F., 1961. The velocity of compressional waves in rocks to 10 kilobars. Pt. 2. J. geophys. Res. 66 (7), 2199–2224.
Blakely, R.J., Brocher, T.M., Wells, R.E., 2005. Subduction zone magnetic anomalies and implications for hydrated forearc mantle. Geology 33 (6), 445–448. https://doi.org/10.1130/G21447.1.
Christensen, N.I., 1966. Elasticity of ultrabasic rocks. Journ. Geophys. Res. v. 71 (N 24), 5921–5931.
Cloetingh, S., Spadini, G., Van Wees, J.D., Beekman, F., 2003. Thermomechanical modelling of Black SeaBasin (de)formation. Sediment. Geol. 156, 169–184.
Clowes, R.M., Hyndman, R.D., 2002. Geophysical studies of the northern Cascadia subduction zone off western Canada and their implications for great earthquake seismotectonics: a review. In: Fujinawa, Y., Yoshida, A. (Eds.), Seismotectonics in Convergent Plate Boundary. Terra Scientific Publishing Company, Tokyo, pp. 1–23.
Contreras-Reyes, E., Grevemeyer, I., Flueh, E.R., Reichert, C., 2008. Upper lithospheric structure of the subduction zone offshore of southern Arauco peninsula, Chile, at ~38◦ S. J. geophys. Res. 113, B07303 https://doi.org/10.1029/2007JB005569.2008.
Cousins, T., Wrobel-Daveau, J.-C., 2018. Frontier exploration in the Eastern Black Sea - the Maria-1 prospect. Exploration Insights, November 2018, 23–31.
Davis, P., Slack, P., Dahlheim, H.A., Green, W.V., Meyer, R.P., Achauer, U., Glahn, A., Granet, M., 1993. Teleseismic tomography of continental rift zones. In: Iyer, H.M., Hirahara, K. (Eds.), Seismic Tomography: Theory and Practice. Chapman and Hall, London, pp. 397–439.
Dercourt, J., Ricou, L.E., Vrielynck, B. (Eds.), 1993. Atlas Tethys Paleoenvironmental Maps. Gauthier-Villars, Paris.
Dercourt, J., Gaetani, M., et al., 2000. Peri-Tethys Palaeogeographical Atlas. Gauthier-Villars, Paris.
Entezar-Saadat, V., Motavalli-Anbaran, S.-H., Jamasb, A., Zeyen, H., 2020. A comprehensive lithospheric study of Black Sea using thermal modeling and

simultaneous joint 3D inversion of potential field data. Tectonophysics 779, 228385. https://doi.org/10.1016/j.tecto.2020.228385.
Ferraccioli, F., Jones, P.C., Vaughan, A.P., Leat, P.T., 2006. New aerogeophysical view of the Antarctic Peninsula: more pieces, less puzzle. Geophys. Res. Lett. 33. https://doi.org/10.1029/2005GL024636.
Finetti, I., Bricchi, G., Pipan, M., Xuan, Z., 1988. Geophysical study of the Black Sea. Bolletino di Geofisica Teorica ed Applicata v. XXX (N117–118), 197–324.
Finn, C., 1994. Aeromagnetic evidence for a buried Early Cretaceous magmatic arc, northeast Japan. J. Geophys. Res. 99, 22165–22185. https://doi.org/10.1029/94JB00855.
Furlong, K.P., Fountain, D.M., 1986. Continental crustal underplating: thermal considerations and seismic-petrologic consequences. J. Geophys. Res.: Solid Earth 91 (B8). https://doi.org/10.1029/JB091iB08p08285.
Garrett, S.W., 1990. Interpretation of reconnaissance gravity and aeromagnetic surveys of the Antarctic Peninsula. J. Geophys. Res. 95, 6759–6777.
Gobarenko, V., Yegorova, T., 2020a. Seismicity and crustal structure of the Southern Crimea and adjacent Northern Black Sea from local seismic tomography. In: Yanovskaya, T.B., et al. (Eds.), Problems of Geocosmos—2018. Springer Proceedings in Earth and Environmental Sciences 215–227. https://doi.org/10.1007/978-3-030-21788-4_18.
Gobarenko, V.S., Yegorova, T.P., 2020b. Seismic tomography model for the crust of Southern Crimea and adjacent Northern Black Sea. J. Volcanol. Seismol. 14 (3), 187–203. https://doi.org/10.1134/S0742046320030033.
Gobarenko, V., Yegorova, T., Stephenson, R., 2017. Local tomography model of the northeast Black Sea: intraplate crustal underthrusting. In: Sosson, M., Stephenson, R. A., Adamia, S.A. (Eds.), Tectonic Evolution of the Eastern Black Sea and Caucasus, 428. Geological Society, London, pp. 228–239. https://doi.org/10.1144/SP428.2 (Special Publications).
Gobarenko, V.S., Yanovskaya, T.B., 2011. The velocity structure of the upper mantle levels of the Black Sea basin,(in Russian). Geophys. J. 33 (3), 62–74.
Golonka, J., 2004. Plate tectonic evolution of the southern margin of Eurasia in the Mesozoic and Cenozoic. Tectonophysics 381, 235–273. https://doi.org/10.1016/j.tecto.2002.06.004.
Gonchar, V.V., 2013. Collisional model of Crimea orogen - investigation by finite elements method. Geophys. J. 35 (6), 146–164.
Gordienko, V.V., Gordienko, I.V., Zavgorodnayay, O.V., Usenko, O.V., 2002. Heat Flow Field of the Territory of Ukraine, Znanie Ukraini, Kiev, p. 170 (in Russian).
Görür, N., 1988. Timing of opening of the Black Sea basin. Tectonophysics 147 (3–4), 247–262.
Graham, R., Kaymakci, N., Horn, B.W., 2013. The Black Sea: something different? GeO ExPro. October 58–62.
Grad, M., Tiira, T., the ESC Working Group, 2009. The Moho depth map of the European Plate. Geophys. J. Int. 176, 279–292.
Grow, J.A., Bowin, C.O., 1975. Evidence for high-density crust and mantle beneath the Chile Trench due to descending lithosphere. J. Geophys. Res. 80, 1449–1458. https://doi.org/10.1029/JB080i011p01449.
Hässig, M., Moritz, R., Ulianov, A., Popkhadze, N., Galoyan, G., Enukidze, O., 2020. Jurassic to Cenozoic magmatic and geodynamic evolution of the Eastern Pontides and Caucasus belts, and their relationship with the Eastern Black Sea Basin opening. e2020TC006336 Tectonics 39. https://doi.org/10.1029/2020TC006336.
Hippolyte, J.-C., 2002. Geodynamics of Dobrogea (Romania): new constraints on the evolution of the Tornquist-Teisseyre Line, the Black Sea and the Carpathians. Tectonophysics 357, 33–53.
Hippolyte, J.-C., Murovskaya, A., Volfman, Yu, Yegorova, T., Gintov, O., Kaymakci, N., Sangu, E., 2018. Age and geodynamic evolution of the Black Sea Basin: Tectonic evidences of rifting in Crimea. Mar. Petrol. Geol. 93, 298–314. https://doi.org/10.1016/j.marpetgeo.2018.03.009.
Hunt, C.P., Moskowitz, B.M., Banerjee, S.K., 1995. Magnetic properties of rocks and minerals. In: Ahrens, T.J. (Ed.), Rock Physics & Phase Relations: A Handbook of Physical Constants, AGU Reference Shelf, Volume 3. American Geophysical Union, pp. 189–204. https://doi.org/10.1029/RF003p0189.
Kaban, M.K., Tesauro, M., Cloetingh, S., 2010. An integrated gravity model for the Europe's crust and upper mantle. Earth Planet. Sci. Lett. 296, 195–209.
Kamiya, S., Kobayashi, Y., 2000. Seismological evidence for the existence of serpentinized wedge mantle. Geophys. Res. Lett. 27, 819–822.
Kornev, O.S., 1982. Anomalies and structures of the Azov-Black-Sea region. Geotectonika 3, 86–97.
Kutas, R.I., Poort, J., 2008. Regional and local geothermal conditions in the northern Black Sea. Int. J. Earth Sci. 97 (2), 353–363.
Kutas, R.I., Kobolev, V.P., Tsvyashchenko, V.A., 1998. Heat flow and geothermal model of the Black Sea depression. Tectonophysics 291, 91–100.
Lavier, L., Manatschal, G., 2006. A mechanism to thin the continental lithosphere at magma-poor margins. Nature 440, 324–328. https://doi.org/10.1038/nature04608.
Letouzey, J., Biju-Duval, B., Dorkel, A., Gonnard, R., Krischev, K., Montadert, L., Sungurlu, O., 1977. The Black Sea: a marginal basin: geophysical and geological data. In: Biju-Duval, B., Montadert, L. (Eds.), Structural History of the Mediterranean Basins. Editions Technip, Paris, pp. 363–376.
Li, L., Clift, P.D., Stephenson, R., Nguyen, H.T., 2014. Non-uniform hyper-extension in advance of seafloor spreading on the Vietnam continental margin and the SW South China Sea. Basin Res. 26, 106–134. https://doi.org/10.1111/bre.12045.
Li, S.Z., Zhao, G.C., Santosh, M., Liu, X., Dai, L.M., 2010. Palaeoproterozoic tectonothermal evolution and deep crustal processes in the Jiao-Liao-Ji Belt, North China Craton: a review. Geol. J. 46, 525–543. https://doi.org/10.1002/gj.1282.
Ludwig, W.J., Nafe, J.E., Drake, C.L., 1970. Seismic refraction. In: Maxwell, A.E. (Ed.), The Sea, v. 4. Wiley-Interscience, New York, pp. 53–84.
Lundin, E.R., Dore, A.G., 2011. Hyperextension, serpentinization, and weakening: a new paradigm for rifted margin compressional deformation. Geology 39, 347–350. https://doi.org/10.1130/G31499.1.
Makris, J., Ginzburg, A., 1987. The Afar Depression: transition between continental rifting and sea-floor spreading. Tectonophysics 141, 199–214.
Malovitsky, Y.P., Neprochnov, Yu.P., et al., 1969. The structure of the Earth's crust in the western part of the Black Sea. Dokl. Akad. Nauk SSSR 186, 905–907.
Malovitsky, Y.P., Uglov, B.D., Osipov, G.V., 1972. Some features of the deep structure of the Black Sea Basin according to hydromagnetic survey. In: Mar. Geol. Geophys., 3. ONTI VIEMS, Moscow, pp. 12–21.
Maynard, J.R., Errat, D., 2020. The Black Sea, a Tertiary basin: observations and insights. Mar. Petrol. Geol. 118, 104462 https://doi.org/10.1016/j.marpetgeo.2020.104462.
Meijers, M.J.M., Vrouwe, B., van Hinsbergen, D.J.J., Kuiper, K.F., Wijbrans, J., Davies, G. R., Stephenson, R.A., Kaymakci, N., Matenco, L., Saintot, A., 2010. Jurassic arc volcanism on Crimea (Ukraine): implications for the paleosubduction zone configuration of the Black Sea region. Lithos 119, 412–426. https://doi.org/10.1016/j.lithos.2010.07.017.
Mileyev, V.S., Rozanov, S.B., Baraboshkin, E.Yu, Rogov, M.A., 2006. Cimmerian and Alpine tectonics of Gorny Crimea. Byulleten Moskovskogo Obshestva Ispytatelei Prirody. Geologia 81 (3), 22–33.
Mileyev, V.S., Vishnevskii, L.E., Nikishin, A.M., Rozanov, S.B., 1992. Formations associated to the accretionary prism of Gorny Crimea. Izv. Vyssh. Uchebn. Zaved., Geol. Razved. 4, 25–31.
Monteleone, V., Minshull, T.A., Marin-Moreno, H., 2019. Spatial and temporal evolution of rifting and continental breakup in the Eastern Black Sea Basin revealed by long-offset seismic reflection data. Tectonics 38, 2646–2667. https://doi.org/10.1029/2019TC005523.
Moskalenko, V.N., Malovitsky, Y.P., 1974. Results of deep seismic sounding along the transmeridional profile across the Azov and Black Seas. Izvestiya of Academy of Sciences of the USSR. Geol. Ser. 9, 23–31.
Nafe, J.E., Drake, Ch.L., 1963. Physical properties of marine sediments. In: Hill, M.N. (Ed.), The Sea, v. 3. Interscience, New York, pp. 794–815.
Neprochnov, Y.P., Kosminskaya, I.P., Malovitsky, Y.P., 1970. Structure of the crust and upper mantle of the Black and Caspian Seas. Tectonophysics 10, 517–538.
Nikishin, A.M., Korotaev, M.V., Ershov, A.V., Brunet, M.-F., 2003. The Black Sea basin: tectonic history and Neogene–Quaternary rapid subsidence modelling. Sediment. Geol. 156, 149–168. https://doi.org/10.1016/S0037-0738(02)00286-5.
Nikishin, A.M., Okay, A.I., Tüysüz, O., Demirer, A., Amelin, N., Petrov, E., 2015a. The Black Sea basins structure and history: New model based on new deep penetration regional seismic data. Part 1: Basins structure and fill. Mar. Petrol. Geol. 59, 638–655 https://doi.org/0.1016/j.marpetgeo.2014.08.017.
Nikishin, A.M., Okay, A.I., Tüysüz, O., Demirer, A., Wannier, M., Amelin, N., Petrov, E., 2015b. The Black Sea basins structure and history: New model based on new deep penetration regional seismic data. Part 2. Tectonic history and peleogeography. Mar. Petrol. Geol. 59, 656–670 https://doi.org/0.1016/j.marpetgeo.2014.08.018.
Nikishin, A.M., Wannier, M., Alekseev, A.S., Almendiger, O.A., Fokin, P.A., Gabdullin, R. R., Khudoley, A.K., Kopaevich, L.F., Mityukov, A.V., Petrov, E.I., Rubtsova, E.V., 2017. Mesozoic to recent geological history of southern Crimea and the Eastern Black Sea region. In: Sosson, M., Stephenson, R.A., Adamia, S.A. (Eds.), Tectonic Evolution of the Eastern Black Sea and Caucasus, 428. Geological Society, London, pp. 241–264. https://doi.org/10.1144/SP428.1 (Special Publications).
Nikishin, A.M., Ziegler, P.A., Bolotov, S.N., Fokin, P.A., 2011. Late Palaeozoic to Cenozoic evolution of the Black Sea – southern Eastern Europe region: a view from the Russian Platform. Turkish. J. Earth Sci. 20, 571–634. https://doi.org/10.3906/yer-1005-22.
Nikishin, A.M., Ziegler, P.A., Panov, D.I., Nazarevich, B.P., Brunet, M.-F., Stephenson, R. A., Bolotov, S.N., Korotaev, M.V., Tikhomirov, P., 2001. Mesozoic and Cenozoic evolution of the Scythian Platform-Black Sea-Caucasus domain. In: Ziegler, P.A., Cavazza, W., Robertson, A.H.F., Crasquin-Solau, S. (Eds.), Peri-Tethys Memoir 6. PeriTethyan Rift /Wrench Basins and Passive Margins. Mémoires du Muséum National d'Histoire Naturelle 186, 296–346. https://doi.org/10.1016/S0037-0738(02)00286-5.
Okay, A.I., Nikishin, A.M., 2015. Tectonic evolution of the southern margin of Laurasia in the Black Sea region. Int. Geol. Rev. 57 (5–8), 1051–1076. https://doi.org/10.1080/00206814.2015.1010609.
Okay, A.I., Şengör, A.M.C., Görür, N., 1994. Kinematic history of the opening of the Black Sea and its effect on the surrounding regions. Geology 22, 267–270. https://doi.org/10.1130/0091-7613(1994)022<0267:KHOTOO>2.3.CO;2.
Okay, A.I., Sunal, G., Tüysüz, O., Sherlock, S., Keskin, M., Kylander-Clark, A.R.C., 2014. Low-pressure – high temperature metamorphism during extension in a Jurassic magmatic arc, Central Pontides, Turkey. J. Metamorph. Geol. 32, 49–69 https://doi.org/0.1111/jmg.12058.
Okay, A.I., Tansel, I., Tüysüz, O., 2001. Obduction, subduction and collision as reflected in the Upper Cretaceous-Lower Eocene sedimentary record of western Turkey. Geol. Mag. 138 (2), 117–142.
Osipov, G.V., Svistunov, Yu.I., Terekxov, A.A., 1977. About the probable nature of the Alushta-Batumi Magnetic anomaly in the Black Sea. Geotectonics 1, 74–79.
Pease, V., Drachev, S., Stephenson, R., Zhang, X., 2014. Arctic lithosphere—a review. Tectonophysics 628, 1–25.
Péron-Pinvidic, G., Manatschal, G., Minshull, T.A., Sawyer, D.S., 2007. Tectonosedimentary evolution of the deep Iberia-Newfoundland margins: evidence for a complex breakup history. Tectonics 26, TC2011. https://doi.org/10.1029/2006TC001970.
Péron-Pinvidic, G., Manatschal, G., 2009. The final rifting at deep magma-poor passive margins from Iberia-Newfoundland: a new point of view. Int. J. Earth Sci. 98, 1581–1597. https://doi.org/10.1007/s00531-008-0337-9.

Popov, D.V., Brovchenko, V.D., Nekrylov, N.A., Plechov, P.Yu, Spikings, R.A., Tyutyunnik, O.A., Krigman, L.V., Anosova, M.O., Kostitsyn, Yu.A., Soloviev, A.V., 2018. Removing a mask of alteration: Geochemistry and age of the Karadag volcanic sequence in SE Crimea. Lithos 324–325, 371–384. https://doi.org/10.1016/j.lithos.2018.11.024.

Prodehl, C., Mueller, St, Glahn, A., Gutscher, M., Haak, V., 1992. Lithospheric cross-sectins of the European Central rift system. Tectonophysics 208, 113–138.

Renner, R.G.B., Dikstra, B.J., Martin, J.L., 1982. Aeromagnetic surveys over the Antarctic Peninsula. In: Craddock, C. (Ed.), Antarctic Geoscience. University of Wisconsin Press, Madison, pp. 363–367.

Robinson, A.G., Kerusov, E., 1997. Stratigraphic and structural development of the Gulf of Odessa, Ukrainian Black Sea: implications for petroleum exploration. In: Robinson, A.G. (Ed.), Regional and Petroleum Geology of the Black Sea and Surrounding Region. AAPG Memoir 68, 369–380.

Robinson, A., Rudat, J.H., Banks, C.J., Wiles, R.L.F., 1996. Petroleum geology of the Black Sea. Mar. Petrol. Geol. 13, 195–223.

Saintot, A., Stephenson, R.A., Chalot-Prat, F., 2007. The position of Crimea and Greater Caucasus along the active margin of Eurasia (from early Jurassic to present). International Symposium on the Middle East Basins Evolution. Abstract, p. 69. Paris. 4–5 December, 2007.

Saintot, A., Stephenson, R.A., Stovba, S., Brunet, M.-F., Yegorova, T., Starostenko, V., 2006a. The evolution of the southern margin of Eastern Europe (Eastern European and Scythian platforms) from the latest Precambrian-Early Palaeozoic to the Early Cretaceous. In: Gee, D.G., Stephenson, R.A. (Eds.), European Lithosphere Dynamics, 32. Geological Society, London, pp. 481–505 (Memoirs).

Saintot, A., Brunet, M.-F., Yakovlev, F., Sébrier, M., Stephenson, R., Ershov, A., Chalot-Prat, F., McCann, T., 2006b. The Mesozoic–Cenozoic tectonic evolution of the Greater Caucasus. In: Gee, D.G., Stephenson, R.A. (Eds.), European Lithosphere Dynamics, 32. Geological Society, London, pp. 277–289 (Memoirs).

Saltus, R.W., Hudson, T.L., Connard, G.G., 1999. A new magnetic view of Alaska. GSA Today 9 (3), 2–6.

Săndulesku, M., 1994. Overview on Romanian geology. In: Berza, T. (Ed.), Alcapa II Field Guidebook: Geological Evolution of the Alpine-Carpathian-Pannonian System, 74. Romanian Journal of Tectonics and Regional Geology, pp. 3–15.

Scott, C.L., Shillington, D.J., Minshull, T.A., Edwards, R.A., Brown, P.J., White, N.J., 2009. Wide-andle seismic data reveal extensive overpressures in the Eastern Black Sea Basin. Geophys. J. Int. 178, 1145–1163. https://doi.org/10.1111/j.1365-246X.2009.04215.x.

Seghedi, A., Oaie, G., 1994. Tectonic setting of two contrasting types of pre-alpine basement: North versus Central Dobrogea. Roman. J. Tectonics Regional Geol. 75, 56–57.

Shillington, D.J., Minshull, T.A., Edwards, R.A., White, N., 2017. Crustal structure of the Mid Black Sea High from wide-angle seismic data. In: Simmons, M.D., Tari, G.C., Okay, A.I. (Eds.), Petroleum Geology of the Black Sea, 464. Geological Society, London, pp. 19–32 https://doi.org/0.1144/SP464.6.

Shillington, D.J., Scott, C.L., Minshull, T.A., Edwards, R.A., Brown, P.J., White, N., 2009. Abrupt transition from magma-starved to magma-rich rifting in the eastern Black Sea. Geology 37 (1), 7–10 https://doi.org/0.1130/G25302A.1.

Shniukova, E.Ye, 2019. Subduction- related magmatism of the Southern Crimea: offshore and onshore. Geol. Miner. Resour. Oceans 15 (3), 3–24.

Shreider, A.A., Kazmin, V.G., Lugin, V.S., 1997. Magnetic anomalies and problem of the age of Black Sea. Geotectonika 1, 59–70.

Simmons, M.D., Tari, G.C., Okay, A.I., 2018. Petroleum geology of the Black Sea: introduction. In: Simmons, M.D., Tari, G.C., Okay, A.I. (Eds.), Petroleum Geology of the Black Sea, 464. Geological Society, London, pp. 1–18. https://doi.org/10.1144/SP464.15.

Sosson, M., Stephenson, R., Sheremet, Ye, Rolland, Ya, Adamia, Sh, Melkonian, R., Kangarli, T., Yegorova, T., Avagyan, A., Galoyan, G., Danielian, T., Hässig, M., Meijers, M., Müller, C., Sahakyan, L., Sadradze, N., Alania, V., Enukidze, O., Mosar, J., 2016. The eastern Black Sea – Cauacasus Region during the Cretaceous: New evidence to constrain its tectonic evolution. Comptes Rendus Geosci. 348 (1), 23–32.

Spadini, G., Robinson, A., Cloetingh, S., 1996. Western versus Eastern Black Sea tectonic evolution: pre-rift lithospheric controls on basin formation. Tectonophysics 266, 139–154.

Spiridonov, E.M., Fedorov, T.O., Ryakhovsky, V.M., 1990a. Magmatic complexes of the Crimean Mountains: paper 1. Byull. Mosk. Obshch. Ispyt. Prirody Otd. Geol. 65 (4), 119–134.

Spiridonov, E.M., Fedorov, T.O., Ryakhovsky, V.M., 1990b. Magmatic complexes of the Crimean Mountains: paper 2. Byull. Mosk. Obshch. Ispyt. Prirody Otd. Geol. 65 (6), 102–112.

Starostenko, V.I., Dolmaz, M.N., Kutas, R.I., Rusakov, O.M., Oksum, E., Hisarli, Z.M., Okyar, M., Kalyoncuoglu, Y., Tutunsatar, H.E., Legostaeva, O.V., 2014. Thermal structure of the crust in the Black Sea: comparative analysis of magnetic and heat flow data. Mar. Geophys. Res. 35, 345–359. https://doi.org/10.1007/s11001-014-9224-x.

Starostenko, V., Buryanov, V., Makarenko, I., Rusakov, O., Stephenson, R., Nikishin, A., Georgiev, G., Gerasimov, M., Dimitriu, R., Legostaeva, O., Pchelarov, V., Sava, C., 2004. Topography of the crust-mantle boundary beneath the Black Sea Basin. Tectonophysics 381 (1–4), 211–233. https://doi.org/10.1016/j.tecto.2002.08.001.

Stephenson, R., Schellart, W.P., 2010. The Black Sea Back-arc Basin: Insights on Its Origin from Geodynamic Models of Modern Analogues, 340. Geological Society,, London, pp. 11–21 (Special Publications).

Stern, R.J., 2002. Subduction zones. Rev. Geophys. https://doi.org/10.1029/2001RG000108.

Talwani, M., Worzel, J.L., Landisman, L., 1959. Rapid gravity computations for two-dimensional bodies with applications to the Mendocino fracture Zone. J. geophys. Res. 64 (1), 49–59.

Tchernychev, M., Makris, J., 1996. Fast calculations of gravity and magnetic anomalies based on 2-D and 3-D grid approach. In: Proceedings of the SEG 66nd Ann. Internat. Mtd., pp. 1136–1138.

Telford, W.M., Geldart, L.P., Sheriff, R.E., Keys, D.A., 1976. Applied Geophysics. Cambridge University Press, New York, p. 860.

Tesauro, M., Kaban, M., Cloetingh, S., 2009. A new thermal and rheological model of the European lithosphere. Tectonophysics 476, 478–495.

Tezcan, A.K., 1995. Geothermal explanation and heat flow in Turkey. In: Gupta, M.L., Yamano, M. (Eds.), Terrestrial Heat Flow and Geothermal Energy in Asia. Oxford and IBH publishing Co Pvt Ltd., New Delhi, pp. 23–42.

Thybo, H., Artemieva, I.M., 2013. Moho and magmatic underplating in continental lithosphere. Tectonophysics 609, 605–619. https://doi.org/10.1016/j.tecto.2013.05.032.

Thybo, H., Nielsen, C.A., 2009. Magma-compensated crustal thinning in continental rift zones. Nature 457, 873–876. https://doi.org/10.1038/nature07688.

Tugolesov, D.A., Gorshkov, A.S., Meisner, L.B., Soloviev, V.V., Khakhalev, V.I., 1985. Tectonics of the Meso-Cenozoic Sediments of the Black Sea Basin. Nedra, Moscow, p. 215.

Verzhbitsky, E.V., 2002. Heat flow and the age of the lithosphere in the Black Sea. Okeanologiya 42, 881–887.

Williams, S., Gubbins, D., 2019. Origin of long-wavelength magnetic anomalies at subduction zones. J. Geophys. Res.: Solid Earth 124. https://doi.org/10.1029/2019JB017479.

Wybraniec, S., Zhou, S., Thybo, H., Forsberg, R., Perhuc, E., Lee, M.K., Demianov, G.D., Strakhov, V.N., 1998. New map compiled of Europe's gravity field. EOS, Trans. Am. Geophys. Un. 79, 437–442.

Yanovskaya, T.B., Gobarenko, V.S., Yegorova, T.P., 2016. Subcrustal structure of the Black Sea Basin from seismological data. Izv., Phys. Solid Earth 52 (1), 14–28.

Yegorova, T., Gobarenko, V., 2010. Structure of the Earth's Crust and Upper Mantle of West- and East-Black Sea Basins Revealed from Geophysical Data and Its Tectonic Implications, 340. Geological Society, London, pp. 23–42 (Special Publications).

Yegorova, T.P., Starostenko, V.I., 2002. Lithosphere structure of Europe and Northern Atlantic from regional three-dimensional gravity modelling. Geophys. J. Int. 151, 11–31.

Yegorova, T., Baranova, E.P., Omelchenko, V.D., 2010. The Crustal Structure of the Black Sea from Reinterpretation of Deep Seismic Sounding Data Acquired in the 1960s, 340. Geological Society, London, pp. 43–56. https://doi.org/10.1144/SP340.4.

Yegorova, T., Gobarenko, V., Yanovskaya, T., 2013. Lithosphere structure of the Black Sea from 3-D gravity analysis and seismic tomography. Geoph. J. Int. 193, 287–303. https://doi.org/10.1093/gji/ggs098.

Yegorova, T.P., Baranova, E.P., Gobarenko, V.S., Murovskaya, A.V., 2018. Crustal Structure of the Crimean Mountains along the Sevastopol–Kerch Profile from the results of DSS and local seismic tomography. Geotectonics 52 (4), 468–484. https://doi.org/10.1134/S0016852118040027.

Yegorova, T., Baranova, E., Murovskaya, A., Farfuliak, L., Repina, K., 2020. The crustal structure of the transition from the East Black Sea Basin to the Shatsky Ridge from reinterpretation of existing refraction seismic profiles 14–15-16. Geoinformatics, 11–14 May 2020, Kiev, Ukraine.

Yegorova, T.P., Bakhmutov, V., Janik, T., Grad, M., 2011. Geophysical and petrological models for the lithosphere structure of the Antarctic Peninsula continental margin. Geophys. J. Int. 184, 90–110. https://doi.org/10.1111/j.1365-246X.2010.04867.x.

Zhai, M., Fan, Q., Zhang, H., Sui, J., Shao, J., 2007. Lower crustal processes leading to Mesozoic lithospheric thinning beneath eastern North China: underplaing, replacement and delamination. Lithos 96 (1–2), 36–54. https://doi.org/10.1016/j.lithos.2006.09.016.

Zonenshain, L.P., Le Pichon, X., 1986. Deep basins of the Black Sea and Caspian Sea as remnants of Mesozoic back-arc basins. Tectonophysics 123, 181–211.